

Preequilibrium decay of nuclei with $A \simeq 90$ at excitation energies to 100 MeV

E. Gadioli and E. Gadioli Erba

Istituto di Fisica dell'Università di Milano, Milano, Italia
and Istituto Nazionale di Fisica Nucleare, Sezione di Milano, Milano, Italia

J. J. Hogan

Department of Chemistry, McGill University, Montreal, Quebec, Canada

(Received 6 August 1976)

Calculations have been made of the excitation functions of 28 nuclear reactions induced by 10–100 MeV protons incident upon targets in the mass region, $A = 90$. Eleven of these reactions have mechanistic components arising from the emission of α particles. Similar calculations have been made of the proton and α particle spectra for 62 MeV protons incident on ^{89}Y . The results of all of the calculations have been compared with the appropriate experimental data. The calculations utilize the theoretical framework of the preequilibrium exciton model for nuclear reactions in conjunction with conventional evaporation theory. A number of recent advances in the computation of equilibration and emission rates, state densities, and the nucleon mean free path have all been incorporated. In addition, introduction of a preformation factor allows the inclusion of α particle emission in both the preequilibrium and evaporation stages of the calculation. Agreement between the calculations making use of no freely varying parameters and all of the experimental data is excellent. In particular, the theoretical model has reproduced the excitation functions for both simple (p,n) and complex $(p,4p6n)$ reactions, at proton energies varying over nearly 100 MeV, for peak cross sections of as little as 1 mb to as great as 1000 mb, including the reactions showing the characteristic double humped curve indicative of α particle emission. Equally well reproduced are the differential proton and α particle energy spectra. The characteristics of the reaction model are discussed with particular reference to the consequences of the more recent advances in the theory mentioned above.

NUCLEAR REACTIONS $^{88}\text{Sr}(p, xn)$, $x=3-5$, $(p, p3n)$, $(p, 2pxn)$, $x=1, 3, 4$;
 $^{89}\text{Y}(p, xn)$, $x=1, 3, 4$, (p, pxn) , $x=2-5$; $^{90}\text{Zr}(p, xn)$, $x=1, 2$, $(p, 2pxn)$, $x=1-5$,
 $(p, 3pxn)$, $x=3, 5, 6$, $(p, 4pxn)$, $x=3-6$; ^{89}Y , p and α spectra; $E=10-100$ MeV;
 calculated $\sigma(E)$, E_p , E_α . ^{88}Sr , ^{90}Zr ; enriched target.

I. INTRODUCTION

Several papers, in recent years, have been devoted to the study of the preequilibrium decay of excited nuclei. Among the various models suggested to deal with this reaction mechanism, the exciton model proved useful in reproducing quantitatively the excitation functions and the spectra of particles emitted in reactions proceeding through excited systems at some tens of MeV of energy. The reactions considered have been (n, xn) , (n, p) , (n, α) , (p, xn) , (p, α) , (α, xn) , and (α, xp) . (See Refs. 1 and 2 and references therein.) Lately, Weidenmüller *et al.* have endeavored to give a theoretical justification of this model starting from the statistics of two body matrix elements of the residual interaction.³ In almost all previous papers, however, only the emission of one type of particle at a time has been considered, e.g., neutrons, protons, or α particles. The simultaneous analysis of processes proceeding through the same composite system and populating several different channels is generally lacking. We feel, however, that a detailed and comprehensive analysis of competing processes in reactions induced by projectiles of

widely varying energy is of the greatest importance in a statistical approach like the one encompassed by the exciton model. A second important question concerns the reliability of calculations based on the model and average sets of parameters when cross sections of only a few mb are concerned. Most of the published analyses of experimental data regard cross sections in the range from 10 to several hundred mb. Though in all these cases reasonable fits have been obtained, can we expect that the model gives reasonable results also in the case of much rarer events with cross sections in the range 1–10 mb?

The question is most important in order to extend the applicability of the model to the analysis of reactions proceeding through composite systems at an excitation energy of about 100 MeV where competition of many final channels decreases the cross section of a particular process. It should be remarked that only a few papers concerning the analysis, in the framework of the exciton model, of reactions proceeding through composite nuclei whose excitation energies can reach about 100 MeV have been published.⁴⁻⁷

Some other calculations based on different ap-

proaches gave unsatisfactory results overestimating sometimes the contribution of compound nucleus processes⁹⁻¹⁰ and requiring in some other instances normalization of the calculated cross sections by arbitrary coefficients.^{11,12} In order to inquire carefully into these two points we decided to start a detailed calculation of reactions induced by protons with energy from 10 to 86 MeV on nuclei with mass $A \approx 50, 90, 200$. This first paper reports the results obtained for $A \approx 90$ nuclei. The reactions considered are summarized in Table I.

Since for many of these reactions detailed calculations based on the intranuclear cascade model VEGAS exist^{9,13} the results we have obtained could be compared with these last ones. This comparison showed that the use in both the intranuclear cascade model and the exciton model of nucleon mean free paths evaluated on the basis of Fermi gas model and free nucleon-nucleon cross sections leads one to overestimate the fraction of those processes proceeding through the formation of a compound nucleus thus overestimating the excitation functions of any given process in the region of the maximum. A satisfactory agreement was found, in exciton model calculations, in all the considered cases, by using the longer mean free path suggested by previous analyses of experimental data.^{1,5,14-16}

II. SUMMARY OF PREVIOUS WORK

The data we considered are the excitation functions of the reactions induced by protons on ^{88}Sr , ^{89}Y , and ^{90}Zr summarized in Table I and the spectra of protons and α particles measured by Bertrand and Peelle¹⁷ in the reactions $^{89}\text{Y}(p, xp)$ and $^{89}\text{Y}(p, x\alpha)$ at $E_p = 61.5$ MeV.

We did not consider the results of Sachdev, Porile, and Yaffe⁹ and Saha, Porile, and Yaffe⁸ at proton energies below 30 MeV because, for some unknown reason, their low energy cross sections are likely to be overestimated. We reached this conclusion by comparing the total cross sections measured by Saha *et al.*, in the case of Y induced reactions, at different proton energies [obtained as a sum of their (p, xn) and (p, pxn) cross sections], and the ones obtained by beam attenuation measurements on ^{90}Zr .^{18,19}

In the energy interval $20 \leq E_p \leq 30$ MeV, the total cross section obtained by summing individual cross sections is substantially higher than the one obtained by beam attenuation measurements reaching a maximum of the order of 1850 mb at $E_p \approx 27$ MeV (at this energy the value obtained by interpolating the data reported in Refs. 18 and 19 amounts to ~ 1250 mb). Also the comparison of the cross sections of the reaction $^{89}\text{Y}(p, n)^{89}\text{Zr}$ measured by Saha *et al.* with the ones measured by Birattari *et al.*⁵ shows that in the energy interval $15 \leq E_p \leq 30$ the values measured by Saha *et al.* are substantially higher. We suspect that also the cross sections measured with the same experimental technique by Sachdev *et al.* on ^{88}Sr are overestimated, in this energy range, since at the maximum of the excitation function, $E_p \approx 25$ MeV, the $^{88}\text{Sr}(p, 2n)$ cross section is near in value to the $^{89}\text{Y}(p, 2n)$ cross section and the sum of (p, n) and $(p, 2n)$ cross sections exceeds the value of the total cross section measured by beam attenuation technique. At $E_p \geq 30$ MeV the cross sections measured by Sachdev *et al.* and Saha *et al.* have been corrected by taking into account the recent measurement of the cross section for the monitor reaction $^{65}\text{Cu}(p, pn)^{64}\text{Cu}$ reported by Newton *et al.*²⁰

The maximum correction occurs at $E_p \sim 45$ MeV

TABLE I. Reactions considered in this work.

Reaction	E_{\min} (MeV)	E_{\max} (MeV)	Reference	Reaction	E_{\min} (MeV)	E_{\max} (MeV)	Reference
$^{88}\text{Sr}(p, 3n)$	29	85	9	$^{90}\text{Zr}(p, n)$	9	86	13
$^{88}\text{Sr}(p, 4n)$	42	85	9	$^{90}\text{Zr}(p, 2n)$	19	86	13
$^{88}\text{Sr}(p, 5n)$	60	85	9	$^{90}\text{Zr}(p, 2pn)$	30	86	13
$^{88}\text{Sr}(p, p3n)$	42	85	9	$^{90}\text{Zr}(p, 2p2n)$	12	86	13
$^{88}\text{Sr}(p, 2pn)$	33	85	9	$^{90}\text{Zr}(p, 2p3n)$	24	86	13
$^{88}\text{Sr}(p, 2p3n)$	25	85	9	$^{90}\text{Zr}(p, 2p4n)$	38	86	13
$^{88}\text{Sr}(p, 2p4n)$	33	85	9	$^{90}\text{Zr}(p, 2p5n)$	56	86	13
$^{89}\text{Y}(p, n)$	4	42	5	$^{90}\text{Zr}(p, 3p3n)$	38	86	13
$^{89}\text{Y}(p, n)$	30.5	85	8	$^{90}\text{Zr}(p, 3p5n)$	62	86	13
$^{89}\text{Y}(p, 3n)$	30.5	85	8	$^{90}\text{Zr}(p, 3p6n)$	80	86	13
$^{89}\text{Y}(p, 4n)$	45	85	8	$^{90}\text{Zr}(p, 4p3n)$	50	86	13
$^{89}\text{Y}(p, p2n)$	30.5	85	8	$^{90}\text{Zr}(p, 4p4n)$	38	86	13
$^{89}\text{Y}(p, p3n)$	36.8	85	8	$^{90}\text{Zr}(p, 4p5n)$	44	86	13
$^{89}\text{Y}(p, p4n)$	60	85	8	$^{90}\text{Zr}(p, 4p6n)$	56	86	13
$^{89}\text{Y}(p, p5n)$	66	85	8				

where the values reported by Sachdev *et al.* and Saha *et al.* have been multiplied by a factor 0.85. The considered excitation functions have been analyzed in the past by means of the intranuclear cascade Monte Carlo model,^{8,9,13} based on the VEGAS computer code.²¹ In all the cases the calculation overestimated the measured cross section at the maxima of the excitation function. This result was interpreted as an indication that the VEGAS calculations overestimated the amount of compound nucleus formation at proton incident energies exceeding a few ten MeV. A similar result was found by Hogan¹⁰ in the analysis of the ⁹⁶Mo(*p*, *xn*) reactions (*x* = 1, 2, 3, 4). Hogan also found that the inclusion of refinements in the Monte Carlo calculations like a velocity dependent nucleon-nucleus potential and constraints on nucleon-nucleon interactions (a collision is forbidden if it occurs at a distance less than 0.5 fm from the location of the previous collision^{22,23} improve the agreement between calculated and measured cross sections in the tail region of the excitation functions, while not reducing the disagreement at the maximum.

III. THEORETICAL CALCULATIONS

A. General considerations

The calculations to be described are based on the exciton model and employ the decay rates for particle emission and exciton-exciton interaction reported in previous papers by Gadioli *et al.*,^{1,14-16} and Milazzo Colli and Braga Marcazzan.²⁴ Since in the present work we aim to evaluate very complex reactions we have used a Monte Carlo technique to evaluate the various cross sections. We followed essentially the Monte Carlo calculations developed by Dostrovsky *et al.*²⁵ for the evaporation from the compound nucleus (CN) and included a preequilibrium stage.

As is known in such calculations one requires only the decay rates for the various competing processes to decide at each stage of the deexcitation the probabilities of various processes occurring.

The extraction of a random number allows one to choose the decay mode of the excited system. Once the emission of a particle occurs, the analytical expression of the energy distribution of the particle considered and the value of the maximum of this distribution are required. A second random number allows one to choose a possible energy for the emitted particle and a third one to decide if this process is to be accepted or rejected by comparing the random number with the ratio between the value of the energy distribution for the chosen energy and its maximum value. The gen-

eral procedure is described in detail in Ref. 25 and the inclusion of the preequilibrium stage in the deexcitation sequence represents a straightforward generalization of this method.

The original Dostrovsky *et al.* calculation²⁵ in order to reduce the computing time did not take into account angular momentum effects. The present calculation does not either partly for the same reason and partly because it is difficult to give a reasonable estimate of the spin distribution of the excited nuclei when the excitation energy is shared among a small number of particles and holes. When discussing the results of the calculations we will try to show that the neglect of angular momentum effects has little consequence on the outcome of the calculation, at least in the case of proton induced reactions.

Angular momentum effects are important when the incident particle brings in much more angular momentum than the emitted particle removes. Such a condition could be met if a compound nucleus were created by an incident projectile of 50–90 MeV energy and some low energy nucleons were evaporated leaving a nucleus with an energy of 10–15 MeV and high spin. After these evaporations the emission of α particles could be enhanced. In the present work, in the few cases where such conditions could take place we have not found systematic disagreement between our calculations and the experimental results.

In addition Dostrovsky *et al.* introduced some other simplifying approximations:

(i) the inverse cross sections were evaluated by means of semiclassical expressions. In the case of neutrons:

$$\sigma_n(\epsilon_n) = \pi R_{on}^2 C_n (1 + \beta/\epsilon_n) A^{2/3}, \quad (1)$$

$$C_n = 0.76 + 2.2A^{-1/3}, \quad (2)$$

$$\beta = (2.12A^{-2/3} - 0.05)/C_n \quad (3)$$

and in the case of protons and α particles:

$$\sigma_{p \text{ or } \alpha}(\epsilon_{p \text{ or } \alpha}) = \pi R_{op \text{ or } \alpha}^2 C_{p \text{ or } \alpha} \left(1 - \frac{V_{p \text{ or } \alpha}}{\epsilon_{p \text{ or } \alpha}}\right) A^{2/3}. \quad (4)$$

(ii) only the exponential energy dependence of the residual nucleus level density was considered $\{\rho(U_R)/\exp[2(aU_R)^{1/2}]\}$. These approximations allowed Dostrovsky *et al.* to give an analytical expression for the total decay rates in the evaporative stage thus greatly reducing the computing time. We also retained these approximations in the evaporative stage except one minor modification to be discussed later, but we used a set of parameters different from those suggested by Dostrovsky *et al.* for the semiclassical cross sections. The new parameters have been obtained by comparing (i) the ratios between the total decay

rate for charged particle emission and the total decay rate for neutron emission and, (ii) the average energies of the emitted particles, both calculated by means of the Dostrovsky procedure, with those obtained by means of calculations performed using optical model inverse cross sections and Fermi gas model level density expressions. This comparison allowed derivation of a simple charge and mass dependence of the parameters of (1) and (4), the Coulomb barriers V , and the effective radii, defined as the product $R_0 C^{1/2}$. For the neutron case the effective radius was taken equal to 1.5 fm. The mass dependence of the effective radii for protons and α particles is given in Figs. 1 and 2. The effective Coulomb barriers are given by

$$\begin{aligned} V_p &= (0.107Z + 0.738) \text{ MeV}, \\ V_\alpha &= (0.203Z + 1.951) \text{ MeV}. \end{aligned} \quad (5)$$

For the quantity β appearing in (1) the same values as suggested by Dostrovsky *et al.* have been used.

After these general considerations let us briefly sketch the main features of the calculations by dividing the deexcitation sequence in two main stages: the preequilibrium and the evaporative stage.

B. Preequilibrium decay

1. First chance preequilibrium emissions

The incident proton is assumed to give rise to a simple initial configuration. In most cases, the initial configuration is assumed to be of the $2p-1h$ type. According to the results of a number of investigations, particularly those by Milazzo Colli *et al.*,^{24,26} in a few cases the incident proton may interact with a preformed α particle giving rise to $1p-1\alpha-1\alpha h$ states. The initial states of the excited composite nucleus can decay either by particle emission or exciton-exciton interactions (particle-particle and/or hole-hole interactions).

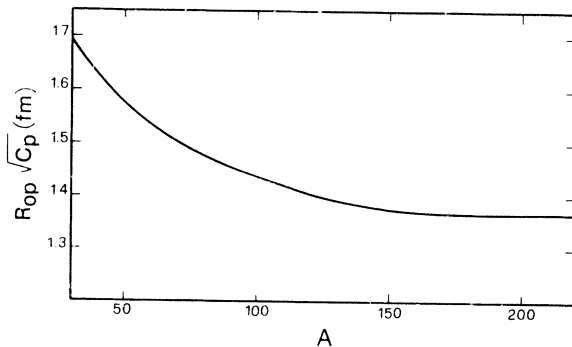


FIG. 1. Mass dependence of the effective proton radius, $R_{0p} C_p^{1/2}$.

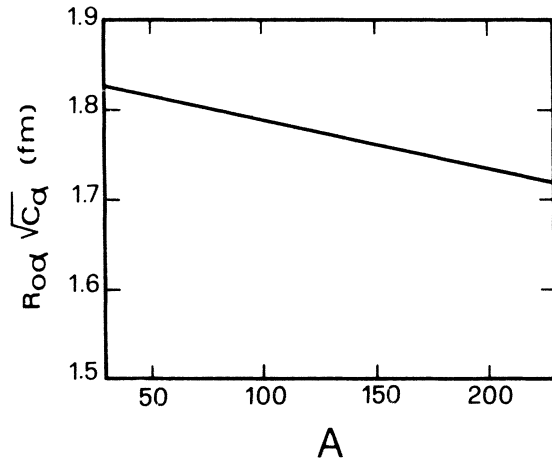


FIG. 2. Mass dependence of the effective alpha radius, $R_{0\alpha} C_\alpha^{1/2}$.

If the latter occurs, the excited composite nucleus reaches a more complicated configuration. The exciton number is generally increased by two units and the competition between the two different decay modes continues. This stage of the reaction process is called the equilibration stage during which preequilibrium decay can occur. Eventually the nucleus reaches a state of statistical equilibrium which further decays by evaporation. Much attention has been paid to the study of particle-particle or hole-hole interactions so that this problem does not require further attention, but the interaction of the α particle or hole with neighboring particles must be discussed. On the basis of the results of the analysis of α particle induced reactions which seem to indicate that in most cases the incident α particle divides into its constituents in the nuclear and Coulomb field of the struck nucleus, we have assumed that in those few instances where an α particle or an α hole are present they interact with other particles or holes like four uncorrelated particles or uncorrelated holes.

In any case, the states characterized by a configuration in which four nucleons are closely correlated to constitute an α particle represent a small minority of the total number of possible states. Therefore the lifetime of the excited composite nucleus at a given stage of the equilibration cascade, characterized by the excitation energy and the number of excitons (when an α particle and an α hole are present they must be counted as two excitons), is only slightly affected by their presence. In order to evaluate the density of the composite nucleus states characterized by a number n of excitons we must recall that: (i) Due to the identity of the projectile not all the configurations corresponding to a given number of parti-

cles and holes are present. (ii) The interaction of a neutron or a proton with a preformed α substructure can occur at any stage of the equilibration cascade. In addition we need to know the density of single α states. We will follow in this paper the widely used procedure of assuming that the density of single α states inside the nucleus is simply one quarter of the density of single nucleon states.^{1,24,26} This simple hypothesis is introduced since in order to cluster into an α particle four nucleons have to be closely correlated. It seems to be supported by analyses of the energy distributions of the α particles emitted in (n, α) and (p, α) reactions which indicate that the density of single α states is really proportional to the density of single nucleon states. However, this assumption can bias the numerical values one obtains for the preformation factor ϕ we introduce below. Indicating then with $\omega_{p,h}(U)$ the total density of states in a p—particle, h—hole configuration at an effective excitation energy U (real excitation energy minus the pairing energy) the density of states of the composite nucleus actually excited will be given in first approximation by²⁴

$$\omega_{p,h}^*(U) = [\phi K_{\alpha}^{p,h} + (1 - \phi) K_n^{p,h}] \omega_{p,h}(U). \quad (6)$$

The coefficients $K_{\alpha}^{p,h}$ and $K_n^{p,h}$ that are given in Table II for different values of p and h ($p+h=n$) take, respectively, into account that (a) in the configurations with one α particle and one α hole there are two excitons with state density one quarter the single nucleon state density that are not identical to the other excited particles and holes; (b) when only nucleon and nucleon holes are excited there are missing configurations according to the point (i) raised above.

An example can help to clarify how these coefficients are calculated. Let us consider a proton induced reaction, as is the case in this paper. Let us assume that the incoming proton interacts with a nucleon. Due to the identity of the projectile the only configurations that can be excited are of

TABLE II. Values of K_n and K_{α} for various pairs of p and h.

p	h	$K_n^{p,h}$	$K_{\alpha}^{p,h}$
2	1	0.375	0.0625
3	2	0.313	0.141
4	3	0.274	0.234
5	4	0.246	0.342
6	5	0.226	0.461
7	6	0.209	0.593
8	7	0.196	0.731
9	8	0.185	0.882
10	9	0.172	1.041
11	10	0.168	1.182

the 2π , $1\pi^-$, and $1\pi^+1\nu$, $1\nu^-$ types (π =proton, π^- =proton hole, ν =neutron, ν^- =neutron hole).

A direct counting of the density of such states shows that it is much less than the total density of $2p$, $1h$ states, when all the possible particle-hole states are excited. In fact $\omega_{(2\pi, 1\pi^-) + (1\pi^+1\nu, 1\nu^-)} = 0.375\omega_{2p, 1h}$.

All the other coefficients reported in Tables II and III are evaluated in a similar way.

The coefficient ϕ represents the probability that a neutron or a proton interacts with a preformed α particle. For simplicity the hypothesis has been introduced that ϕ is independent of the relative energy of the nucleon and the struck α particle. Its value must be deduced, at present state of the model, by the analysis of experimental data. The state densities $\omega_{p,h}(U)$ for $p \leq 7$, $h \leq 6$ have been calculated by means of recursion formulas¹⁴

$$\omega_{p,0}(U_p) = \frac{1}{p} \int_0^{U_p} \omega_{1,0}(u) \omega_{p-1,0}(U_p - u) du,$$

$$\omega_{0,h}(U_h) = \frac{1}{h} \int_0^{U_h} \omega_{0,1}(u) \omega_{0,h-1}(U_h - u) du, \quad (7)$$

$$\omega_{p,h}(U) = \int_0^U \omega_{p,0}(U_p) \omega_{0,h}(U - U_p) dU_p,$$

where u is the particle or hole energy measured from the Fermi energy, U_p and U_h the total excitation energies of particles and holes, $U = U_p + U_h$ is the total energy of the composite nucleus. The single nucleon densities are assumed to be given, for nucleon states with energy lower than the Fermi energy, by the law

$$g(\epsilon) = \frac{3}{2} \frac{A}{\epsilon_f^{3/2}} \epsilon^{1/2} \quad (8)$$

as predicted by Fermi gas model. The Fermi energy ϵ_f is assumed to be equal to 20 MeV in order to reproduce the single nucleon density at the Fermi energy as deduced by the analysis of slow neutron resonance spacings. For nucleon states

TABLE III. Values of K_i for various pairs of p-1, h.

p-1	h	$K_n^{p-1,h}$	$K_p^{p-1,h}$	$K_{\alpha}^{p-1,h}$
1	1	0.500	0.250	0.125
2	2	0.376	0.250	0.188
3	3	0.313	0.235	0.234
4	4	0.273	0.219	0.274
5	5	0.247	0.205	0.308
6	6	0.225	0.193	0.339
7	7	0.209	0.183	0.366
8	8	0.196	0.174	0.392
9	9	0.181	0.163	0.416
10	10	0.176	0.160	0.430

with energy greater than the Fermi energy the single nucleon state density is assumed to be constant and equal to the value predicted by (8) at the Fermi energy. This assumption is based on purely phenomenological considerations which seem to indicate in the case of α particle induced reactions¹ that the expression (8) gives a variation of $g(\epsilon)$ with the energy which increases too rapidly for $\epsilon > \epsilon_f$. However, in our opinion, the whole subject of state densities of few particle-hole states requires further consideration. We recall that an empirical knowledge of the single nucleon

state density mainly refers to states in the proximity of the Fermi energy while in the first stages of the equilibration cascade states with energy much greater or lower than the Fermi energy are involved.

The recursion formulas (7) allow one to take correctly into account the finite depth of the potential well to which nucleon states are confined, but do not account for the restriction imposed by the Pauli principle. For this reason, for $p > 7$, $h > 6$ we evaluated $\omega_{p,h}(U)$ by means of the expression reported by Betak and Dobeš²⁷

$$\omega_{p,h}(U) = g^n \frac{[U - A(p, h)]^{n-1} - h \Theta(U - \alpha_{p,h} - \epsilon_f) [U - A(p, h) - \epsilon_f]^{n-1}}{p! h! (n-1)!}, \quad (9)$$

where

$$A(p, h) = \frac{1}{4g} (p^2 + h^2 + p - 3h)$$

and

$$\alpha_{p,h} = (p^2 + h^2 + p - h) / 2g.$$

$\Theta(x)$ is the Heaviside function, $\Theta(x) = 1$ if $x > 0$, 0 if $x < 0$.

The expression (9) allows one to take into account, in first approximation, both the finite depth of the potential well and the Pauli principle. This formula assumes an equidistant spacing for all nucleon states.

When the emission of one particle occurs the state densities of residual nucleus at the effective excitation energy U_R are, respectively, given by

$$\begin{aligned} \omega_{p-1,h}^{\pi} (U_R) &= (1 - \phi) K_{\pi}^{p-1,h} \omega_{p-1,h}(U_R), \\ \omega_{p-1,h}^{\nu} (U_R) &= (1 - \phi) K_{\nu}^{p-1,h} \omega_{p-1,h}(U_R), \\ \omega_{p-1,h}^{\alpha} &= \phi K_{\alpha}^{p-1,h} \omega_{p-1,h}(U_R), \end{aligned} \quad (10)$$

where the π , ν , and α subscripts denote proton, neutron, and alpha particle, respectively. The coefficients $K_{\pi}^{p-1,h}$, $K_{\nu}^{p-1,h}$, and $K_{\alpha}^{p-1,h}$, which are analogous to the ones appearing in expression (6), are given, for various pairs of $p-1, h$ values, in Table III.

The decay rate for emission of a particle i ($i = \pi, \nu, \alpha$) with energy ϵ_i into the continuum is given by

$$\begin{aligned} W_c^{p,h}(U, \epsilon_i) d\epsilon_i \\ = \frac{1}{\pi^2 \hbar^3} \frac{m_i A_R}{m_i + A_R} \frac{(2s_i + 1)}{\omega_{p,h}^*(U)} \sigma_{\text{inv},i}(\epsilon_i) \epsilon_i \omega_{p-1,h}^*(U_R) d\epsilon_i \end{aligned} \quad (11)$$

and the total decay rate for emission of a particle whichever is the type and the energy is given by

$$W_c^{p,h}(U) = \sum_i \int_0^{\epsilon_i^{\text{max}}} W_c^{p,h}(U, \epsilon_i) d\epsilon_i. \quad (12)$$

In expression (11) m_i and A_R are the particle and residual nucleus masses, s_i the particle spin, and $\sigma_{\text{inv},i}(\epsilon_i)$ the cross section for the inverse process. Since at this stage of the calculations the total decay rates (12) and the maxima of the differential decay rates (11) are computed numerically, in order to achieve a better accuracy, the neutron and proton inverse cross sections have been evaluated by means of the formulas reported in Ref. 15. These inverse cross sections, however, in the range of energies of interest at this stage of the calculations, differ from the values given by expressions (1) and (4) no more than a few percent. In the case of α particles, the inverse cross section is given by (4), with the parameters previously quoted, reduced by 15%, as reported in Ref. 1, to take into account those processes which presumably do not contribute to preequilibrium decay. The competing decay rates for exciton-exciton interactions, $W_{\text{eq}}^{p,h}(U)$, that represent the transition rates to more complicated states, have been reported in previous papers.^{1,14,16,28} For the sake of completeness we report in Table IV, as a function of the excitation energy of the composite nucleus, the numerical values of $W_{\text{eq}}^{p,h}(U)$ for different pairs of p and h values. The present numerical values differ slightly (in no case more than a few percent) from the values previously quoted as a consequence of the present choice of single nucleon state densities.

At the beginning of the Monte Carlo calculations, for each particle considered and each set of p, h values, the decay rates for decay into the continuum have been numerically evaluated. The values of their maxima and of the integral over the emitted particle energy is calculated and stored in the memory. The exciton-exciton interaction

TABLE IV. Decay rates, $W_{e_q}^{p,h}(U)$, for exciton-exciton interactions utilized in present work (the unit of the decay rates is 10^{22} sec^{-1}).

U (MeV)	$W_{e_q}^{2,1}$	$W_{e_q}^{3,2}$	$W_{e_q}^{4,3}$	$W_{e_q}^{5,4}$	$W_{e_q}^{6,5}$	$W_{e_q}^{7,6}$	$W_{e_q}^{8,7}$	$W_{e_q}^{9,8}$	$W_{e_q}^{10,9}$	$W_{e_q}^{11,10}$
3	0.022	0.018	0.012	0.010	0.008	0.006	0.005	0.004	0.003	0.002
5	0.054	0.040	0.034	0.031	0.027	0.022	0.019	0.016	0.014	0.011
10	0.17	0.13	0.11	0.092	0.080	0.072	0.061	0.052	0.044	0.038
15	0.34	0.26	0.22	0.19	0.16	0.15	0.13	0.12	0.11	0.10
20	0.55	0.43	0.35	0.30	0.27	0.24	0.22	0.21	0.20	0.19
25	0.74	0.63	0.52	0.45	0.39	0.35	0.32	0.30	0.29	0.28
30	0.91	0.84	0.71	0.61	0.54	0.48	0.43	0.41	0.39	0.38
35	1.04	1.03	0.91	0.79	0.70	0.63	0.56	0.52	0.50	0.48
40	1.17	1.22	1.12	0.99	0.88	0.79	0.71	0.66	0.62	0.59
45	1.26	1.37	1.31	1.19	1.07	0.96	0.88	0.81	0.75	0.71
50	1.35	1.54	1.51	1.40	1.27	1.15	1.06	0.97	0.90	0.85
55	1.41	1.65	1.67	1.58	1.46	1.34	1.26	1.15	1.07	1.00
60	1.48	1.80	1.86	1.79	1.67	1.55	1.48	1.35	1.25	1.17
65	1.52	1.87	1.99	1.96	1.86	1.74	1.70	1.56	1.44	1.35
70	1.58	2.00	2.16	2.16	2.07	1.95	1.93	1.78	1.65	1.54
75	1.60	2.05	2.26	2.30	2.24	2.14	2.15	2.01	1.86	1.74
80	1.65	2.16	2.41	2.49	2.45	2.35	2.38	2.23	2.09	1.95
85	1.66	2.20	2.49	2.60	2.59	2.52	2.59	2.46	2.31	2.17
90	1.70	2.29	2.63	2.77	2.79	2.73	2.80	2.68	2.54	2.39
95	1.71	2.31	2.68	2.86	2.91	2.88	3.00	2.90	2.76	2.62
100	1.74	2.40	2.81	3.03	3.10	3.09	3.19	3.11	2.98	2.84

decay rates were provided as input data.

The extraction of a sequence of random numbers, following the Dostrovsky *et al.* procedure, allowed us to choose one particular reaction path. This first part of the calculation ends when either a pre-equilibrium particle is emitted or the compound nucleus state is reached. The latter is assumed to have occurred when the exciton number equals $(2gU)^{1/2}$. In the first case the identity and the energy of the emitted particle, the Z and N of the residual nucleus, the excitation energy, the number of excitons which share this excitation energy are stored.

2. Second chance preequilibrium emissions

If a first chance preequilibrium emission occurs, the possibility of second chance emission is considered. If second chance preequilibrium emission

also occurs, the possibility of a third chance emission is considered and so on up to four possible preequilibrium emissions. In order to reduce the computing time, some simplifying approximations are introduced. First, due to the rather weak dependence of $W_{e_q}^n(U)$ on n , the various exciton-exciton decay rates have been substituted by one averaged over n which is calculated by means of a polynomial expansion whose coefficients are given as input data. This decay rate, averaged over n is reported in Fig. 3 as a function of the excitation energy. Second, by introducing the inverse cross sections given by (1) and (4) and the equidistant spacing state density expressions first reported by Ericson²⁹ the maxima of the decay rates for particle emission (11) and their integral over the energy have been computed analytically. A straightforward calculation leads to the following expressions for the total rate of emission of neutrons, protons, and α particles:

$$W_c^n(U)_\nu = \frac{1}{\pi^2 \hbar^3} \frac{m_\nu A}{m_\nu + A} (2S_\nu + 1) \frac{1}{g_{CN}} \left(\frac{g_R}{g_{CN}} \right)^{n-1} \frac{n(n-1)}{2} \pi R_{0\nu}^2 C_\nu A^{2/3} \\ \times \frac{(1-\phi)}{(1-\phi) + \phi(n^2/64)} E_{\max}^\nu \left(\frac{E_{\max}^\nu}{U} \right)^{n-1} \left(\frac{1}{n(n-1)} + \frac{1}{(n-1)} \frac{\beta}{E_{\max}^\nu} \right), \quad (13)$$

$$W_c^n(U)_\pi = \frac{1}{\pi^2 \hbar^3} \frac{m_\pi A}{m_\pi + A} (2S_\pi + 1) \frac{1}{g_{CN}} \left(\frac{g_R}{g_{CN}} \right)^{n-1} \frac{n(n-1)}{2} \pi R_{0\pi}^2 C_\pi A^{2/3} \\ \times \frac{(1-\phi)}{(1-\phi) + \phi(n^2/64)} (E_{\max}^\pi - V_\pi) \left(\frac{E_{\max}^\pi - V_\pi}{U} \right)^{n-1} \frac{1}{n(n-1)}, \quad (14)$$

$$W_c^n(U)_\alpha = \frac{1}{\pi^2 \hbar^3} \frac{m_\alpha A}{m_\alpha + A} \frac{1}{g_{CN}} \left(\frac{g_R}{g_{CN}} \right)^{n-1} \frac{n(n-1)}{2} \pi R_{0\alpha}^2 C_\alpha A^{2/3} \\ \times \frac{\phi_{\frac{1}{8}} n}{(1-\phi) + \phi(n^2/64)} (E_{\max}^\alpha - V_\alpha) \left(\frac{E_{\max}^\alpha - V_\alpha}{U} \right)^{n-1} \frac{1}{n(n-1)}. \quad (15)$$

We have not taken into account the reduction in the number of configurations due to the identity of the projectile [i.e., we put all the K coefficients in expressions like (6) and (10) equal to unity]. The error introduced is likely to be small; in considering second chance preequilibrium emission the ratio of the correct coefficients which multiply the residual and the decaying nuclei level densities in the case of nucleon emission, the most probable occurrence, goes rapidly to unity as the exciton number increases. The quantities E_{\max}^ν , E_{\max}^π and E_{\max}^α are, respectively, the maximum effective excitation energy of the residual nuclei A , g_{CN} is the single nucleon state density for the decaying nuclei and g_R the same for the residual nuclei. The values of the energies at the maxima of the differential decay rates for particle emission are, respectively, for neutron, proton, and α particles:

$$\epsilon_{\max, \nu} = \frac{E_{\max}^\nu - (n-2)\beta}{(n-1)}, \quad (16)$$

$$\epsilon_{\max, \pi} = \frac{E_{\max}^\pi + (n-2)V_\pi}{(n-1)}, \quad (17)$$

$$\epsilon_{\max, \alpha} = \frac{E_{\max}^\alpha + (n-2)V_\alpha}{(n-1)}. \quad (18)$$

According to the considerations of the preceding subsection, after one preequilibrium emission of any particle a second chance α particle emission is possible only if at least one exciton-exciton interaction occurred. Indeed if this interaction did not occur no α particle could be present nor emitted due to the hypothesis that an α particle

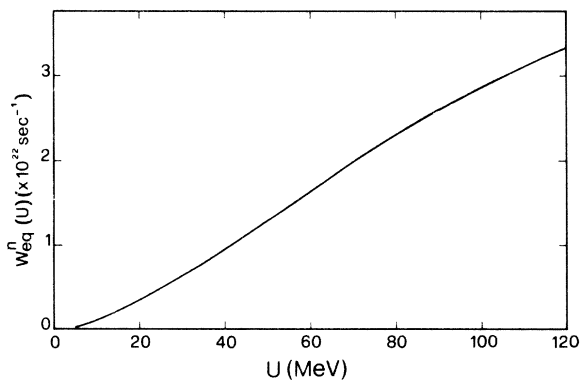


FIG. 3. Variation of the average exciton-exciton interaction decay rate with increasing excitation energy.

does not survive at length inside the nucleus and the probability of clustering of four excited nucleons into an α particle is negligible. After one α particle preequilibrium emission no other preequilibrium emissions are assumed to be likely since the α hole is assumed to behave like four uncorrelated holes thus increasing the exciton number of the excited residual nucleus and reducing the probability of a further preequilibrium emission. Indeed the ratio

$$\frac{\sum_i W_c^n(U)_i}{W_{eq}^n(U)}$$

greatly decreases with increasing exciton number n .

C. Evaporative stage

At the end of the preequilibrium stage an excited nucleus is left. This nucleus deexcites by evaporation. During this stage of the calculation we used essentially the same formulas as employed by Dostrovsky *et al.* except for a single modification.

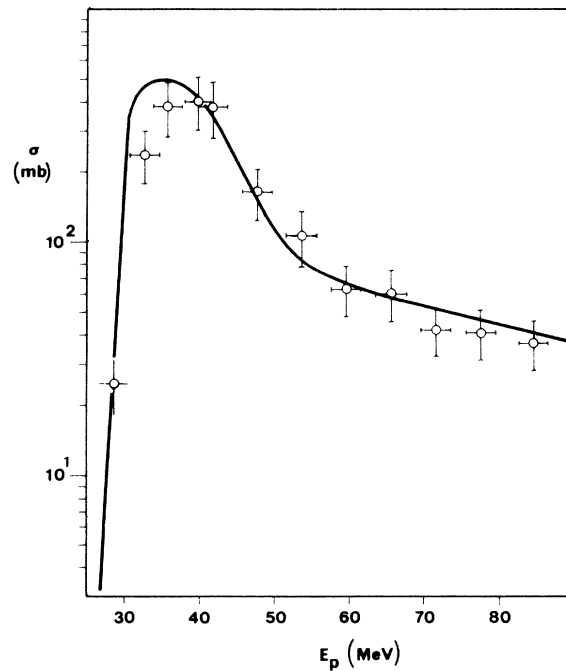


FIG. 4. Comparison of the calculated (full line) and experimental excitation functions for the $^{88}\text{Sr}(p, 3n)$ reaction.

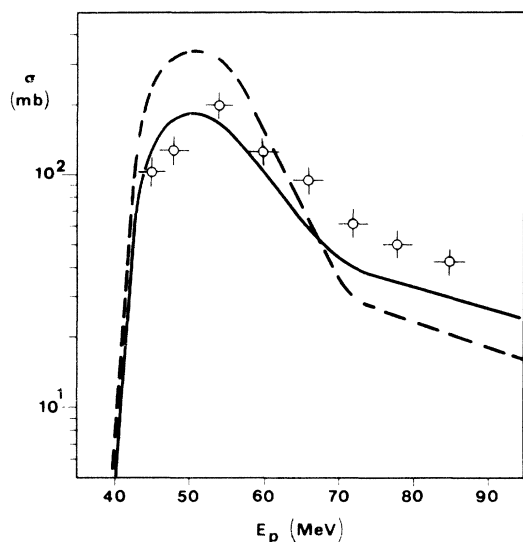


FIG. 5. As Fig. 4, for the $^{88}\text{Sr}(p, 4n)$ reaction. The dashed line represents the results of the calculation with decay rates, $W_{e_q}^n$, increased by a factor of 4 with respect to the values reported in Table IV. See discussion in text.

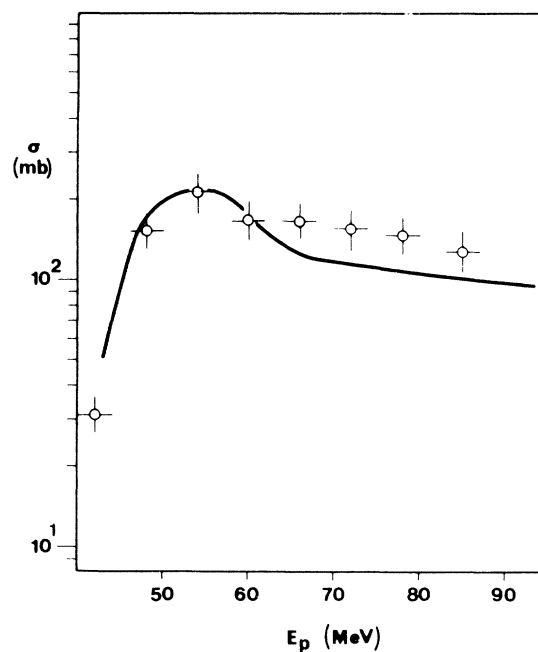


FIG. 7. As Fig. 4, for the $^{88}\text{Sr}(p, p3n)$ reaction.

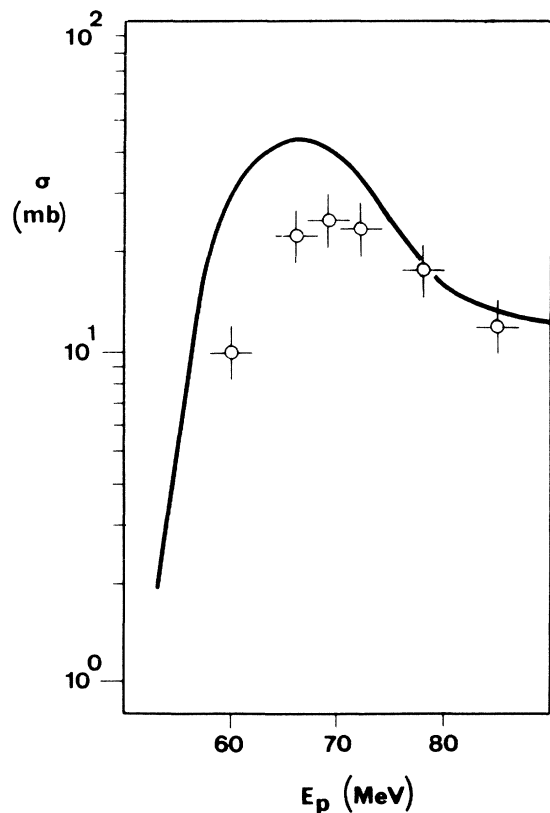


FIG. 6. As Fig. 4, for the $^{88}\text{Sr}(p, 5n)$ reaction.

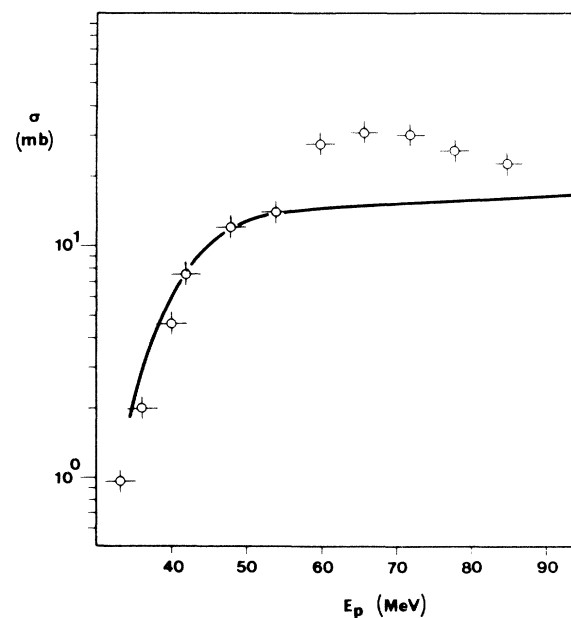
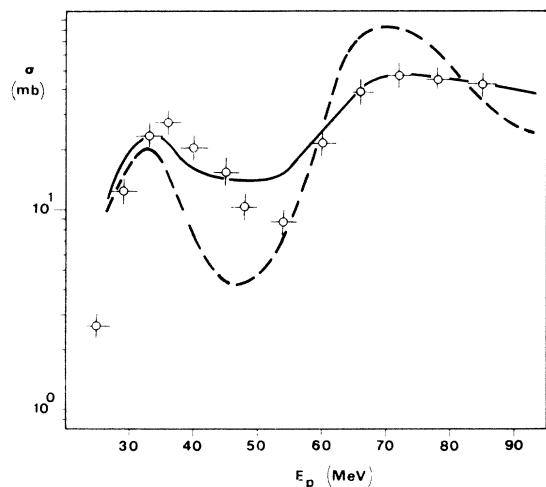


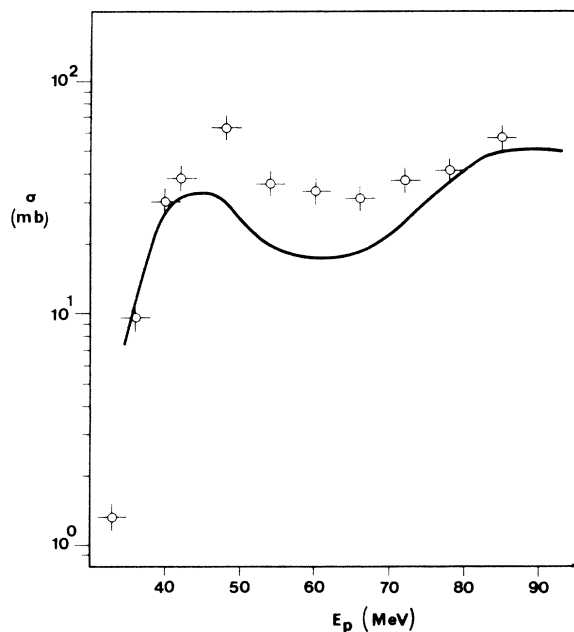
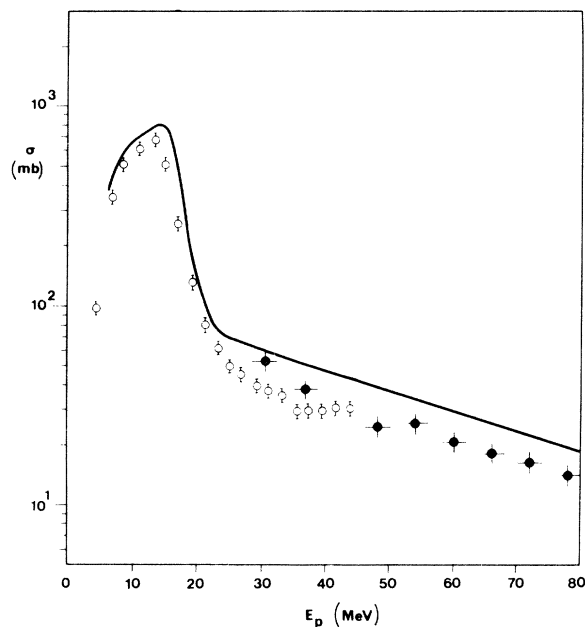
FIG. 8. As Fig. 4, for the $^{88}\text{Sr}(p, 2pn)$ reaction.

As has been previously noted to obtain an analytical expression for the total decay rates these authors have neglected in the expression of the level density $\rho(U)$ the preexponential factor $(U+t)^{-2}$. This approximation forced them to utilize unrealistic values for the level density parameter a appearing in the expression of $\rho(U)$.

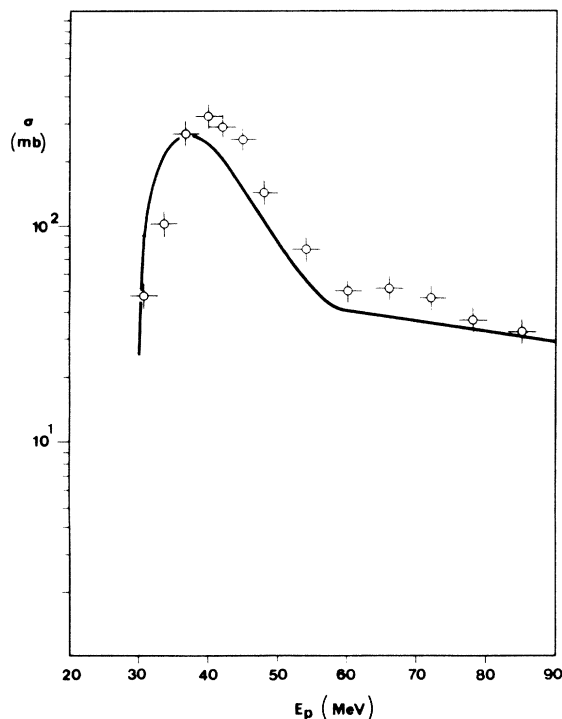
We found a simple way to take approximately into account the preexponential factor, retaining

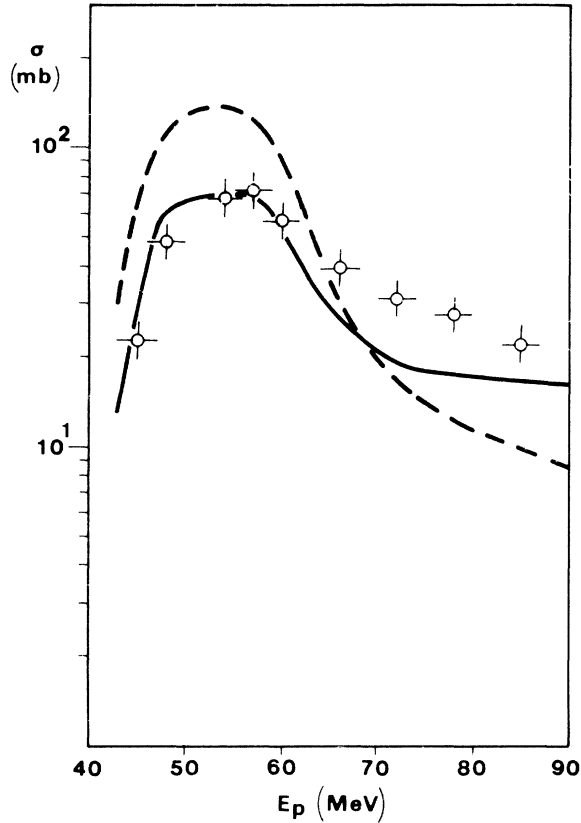
FIG. 9. As Fig. 5, for the $^{88}\text{Sr}(p, 2p3n)$ reaction.

at the same time the great computing advantages of Dostrovsky procedure, that consists in dividing the analytical expressions reported by Dostrovsky *et al.* for the widths corresponding to the emission of the various particles by the square of the average excitation energy of the residual nucleus. According to our calculations, if one appropriately chooses for each considered compound nucleus the proton and α particle Coulomb barriers, these modified expressions allow one to reproduce within a few percent, using the same level density parameters, the ratios between the charged particle and neutron widths and the average kinetic energies of the emitted particles,

FIG. 10. As Fig. 4, for the $^{88}\text{Sr}(p, 2p4n)$ reaction.FIG. 11. As Fig. 4, for the $^{89}\text{Y}(p, n)$ reaction.

numerically evaluated for excitation energies ranging from ~ 15 to ~ 100 MeV by means of the correct Fermi gas model level density and the optical model inverse cross sections. The accuracy is reduced using Coulomb barriers given by simple numerical laws like the (5) previously reported,

FIG. 12. As Fig. 4, for the $^{89}\text{Y}(p, 3n)$ reaction.

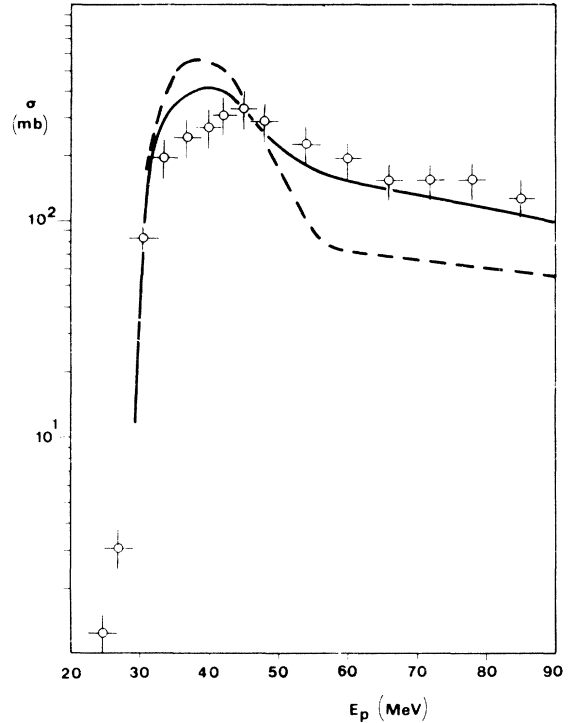
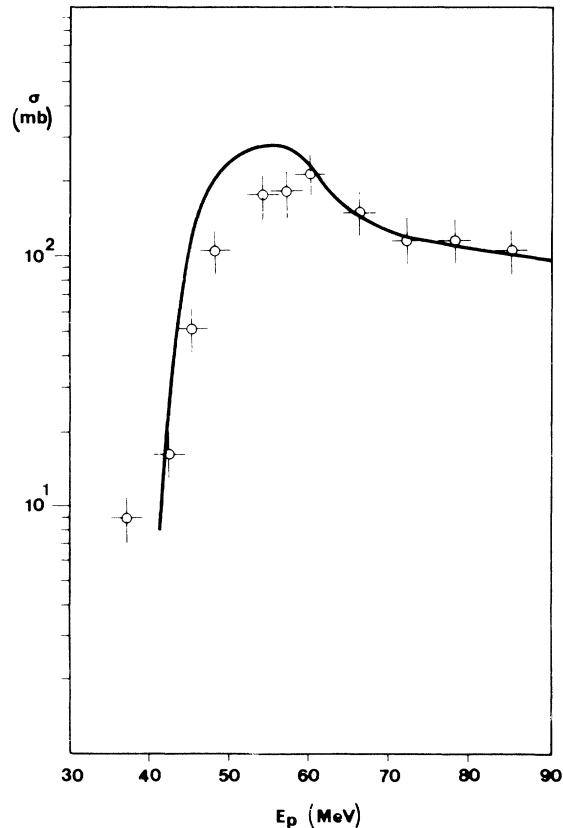
FIG. 13. As Fig. 5, for the $^{89}\text{Y}(p, 4n)$ reaction.

but we estimate that for $50 \leq A \leq 200$ nuclei and for excitation energies in the range considered, the analytically computed ratio between proton and neutron width could differ at most by 20% from the numerical one; in the case of the ratio between α and neutron width the discrepancy could amount to 30%.

We do not report the formulas utilized that, except for the modification introduced, can be found in Dostrovsky *et al.*'s paper to which the reader interested is referred.²⁵ We evaluated the average excitation energy of the residual nucleus as its maximum excitation energy less $2T$ or $(2T + V)$ in the case, respectively, of neutrons or charged particles. We approximated T by $(E_{\text{max}}/a)^{1/2}$ or $[(E_{\text{max}} - V)/a]^{1/2}$, respectively, where E_{max} is the maximum excitation energy and a the level density parameter.

D. Other parameters entering in the calculation

In addition to the parameters quoted in the previous section, the binding energies tabulated by Wapstra and Gove³⁰ have been used. When some of the binding energies were experimentally unknown, they have been calculated by means of the Myers and Swiatecki³¹ semiempirical mass formu-

FIG. 14. As Fig. 5, for the $^{89}\text{Y}(p, p2n)$ reaction.FIG. 15. As Fig. 4, for the $^{89}\text{Y}(p, p3n)$ reaction.

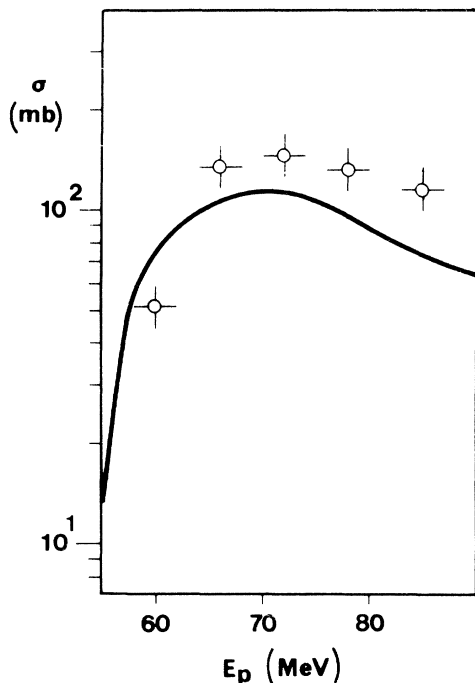


FIG. 16. As Fig. 4, for the $^{89}\text{Y}(p, p4n)$ reaction.

1a. The pairing energies have been taken from Nemirovski and Adamchuck.³² In the evaporative stage the level density parameter $a = A/8 \text{ MeV}^{-1}$ has been utilized. This choice corresponds to the previous one of a value of the Fermi energy equal to 20 MeV in the expression of the single nucleon state density. To conclude this subsection we wish to stress that if one excludes the probability ϕ for a nucleon to strike a preformed α particle, no free parameters are introduced in the calculations.

Since most of the parameters utilized are average values which cannot take into account individual properties of the nuclei involved in the deexcitation process one must not expect in all the cases considered a very detailed fit of the experimental data and some deviations (that, however, should not alter essentially the conclusions one should draw from the comparison of the calculations and the experimental findings) are expected.

IV. COMPARISON OF THE EXPERIMENTAL DATA WITH THEORETICAL CALCULATIONS AND DISCUSSION

In Figs. 4–17 comparisons between the experimental excitation functions reported in Table I for protons incident upon ^{88}Sr (Ref. 9) and ^{89}Y (Ref. 8) and the theoretical calculations (in all cases the full line) are shown. In Figs. 18 and 19 the comparison between the calculated proton and α spectra and the ones measured by Bertrand and Peelle¹⁷ in proton bombardment of ^{89}Y is shown. In Figs. 20–33 the comparison between theory and

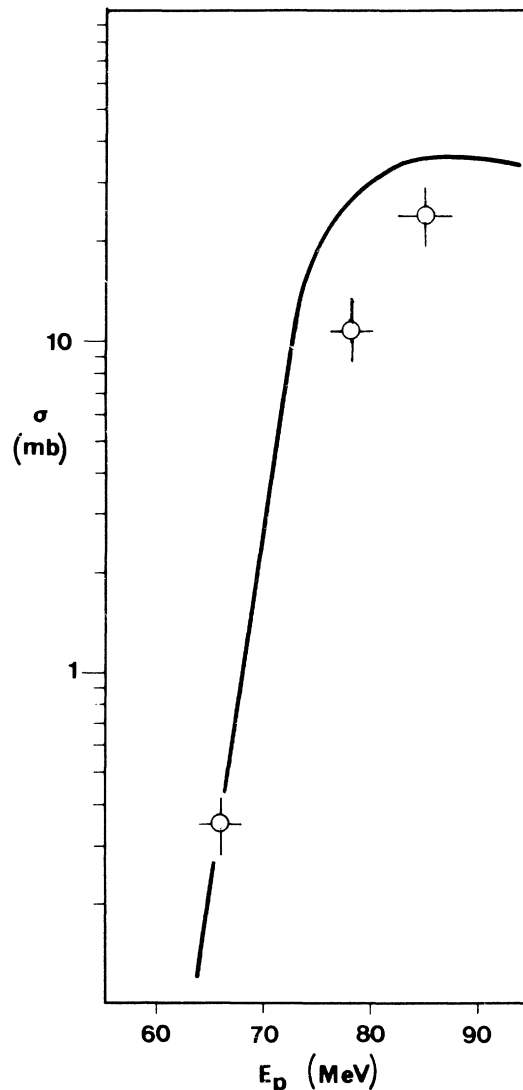


FIG. 17. As Fig. 4, for the $^{89}\text{Y}(p, p5n)$ reaction.

experiment in the case of the excitation functions of the reactions induced in ^{90}Zr (Ref. 13) is reported. Before undertaking a fuller discussion of the data we draw some general conclusions.

(i) Without noticeable exceptions the rise of the excitation functions is satisfactorily reproduced in all cases, even at high energies. This fact seems to confirm the validity of the approximations that have been introduced when calculating the inverse cross sections and provides an *a posteriori* justification of the neglect of angular momentum effects.

(ii) The neutron, proton, and α decay modes seem to be reproduced in an equivalent way without systematic deviations in one or the other sense.

(iii) The agreement between experimental data and the theoretical calculations is, in general, satisfactory both at the maxima and at the tails of the excitation functions. This essentially means

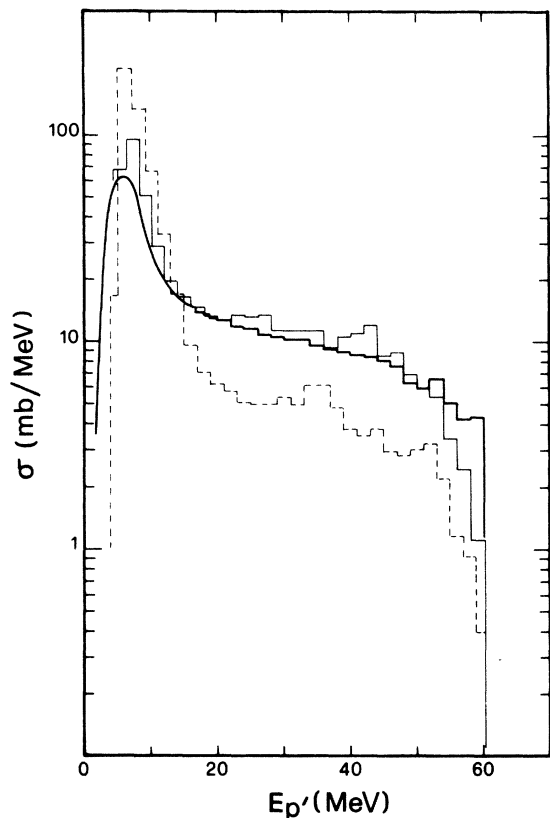


FIG. 18. Comparison of the experimental spectrum of protons emitted in the 61.5 MeV proton bombardment of ^{89}Y with the calculated spectrum. The broad line represents the experimental data; the narrow solid line is the calculated histogram. The dashed line is the calculated value with the decay rates increased by a factor of 4 with respect to the values reported in Table IV. See discussion in text.

that the contributions due to preequilibrium decay and compound nucleus evaporation are both reasonably reproduced.

(iv) The agreement between theoretical calculations and experimental data seems to be comparatively better in the case of very complex reactions with cross sections of a few mb. This fact constitutes a proof of the essential validity of the average parameters utilized and of the absence of systematic deviations of the theoretical calculations from the experimental findings.

A. Analysis of ^{88}Sr excitation functions

The shape and the absolute value of the (p, xn) excitation functions ($x=3, 4, 5$) is satisfactorily reproduced. Only in the case of the $(p, 5n)$ reaction is the maximum of the excitation function somewhat overestimated ($\approx 30\%$). The agreement of experimental data and calculations is very satisfactory in the case of the $(p, p3n)$ reaction [at

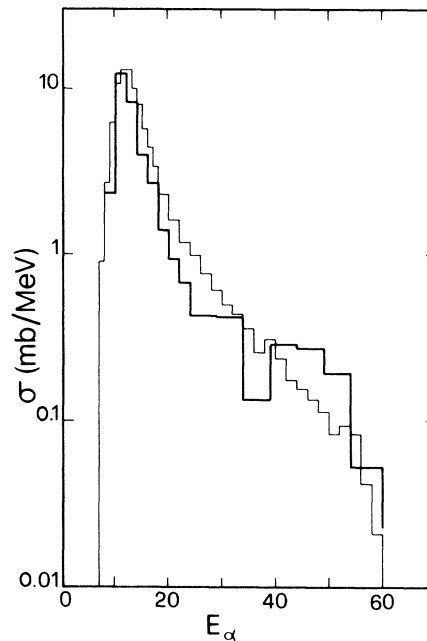


FIG. 19. Comparison of measured (narrow solid line) and calculated (broad solid line) α spectrum in ^{89}Y (p, α) reaction at $E_p = 61.5$ MeV.

the highest energies the calculated excitation function slightly underestimates the experimental one; this is presumably due to the fact that the calculations neglect the contribution of the $(p, d2n)$ reaction].

In the case of the $(p, 2pn)$ reaction the calculations reproduce satisfactorily the experimental data up to ≈ 55 MeV incident proton energy. At higher energies the calculated excitation function underestimates the measured one. At present we have not found reasons to explain this discrepancy. The $(p, 2p3n)$ and $(p, 2p4n)$ excitation functions show a first maximum which has to be attributed to the reactions $(p, \alpha n)$ and $(p, \alpha 2n)$. Beyond this maximum, in the energy range considered, a valley follows and a further rise when the emission of, respectively, $2p$ and $3n$ and $2p$ and $4n$ becomes energetically possible. In both cases the shape of the experimental excitation functions is satisfactorily reproduced. The absolute value of the $(p, 2p3n)$ excitation function is well reproduced by assuming for the ϕ factor the value 0.1. With this choice the $(p, 2p4n)$ excitation function is somewhat underestimated at the first maximum and the valley. A better agreement would be obtained by assuming $\phi \approx 0.15$.

We do not attribute a great significance to this slight discrepancy; in particular, we do not think that the energy spectrum of the α particle which is presumably the first particle emitted in both reac-

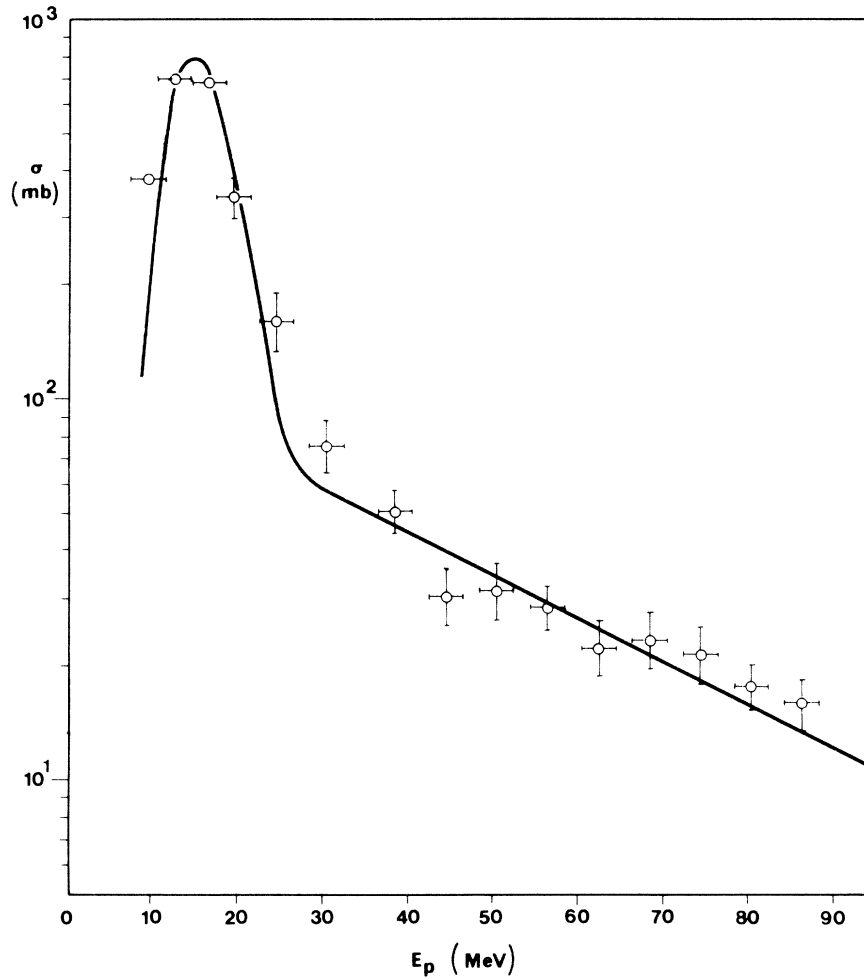


FIG. 20. As Fig. 4, for the $^{90}\text{Zr}(p, n)$ reaction.

tions is badly reproduced. In fact in the case of the reactions induced on ^{90}Zr (see later) with the same ϕ value for both reactions the situation is reversed: The $(p, 2p3n)$ reaction is slightly underestimated at the first maximum and the valley while the $(p, 2p4n)$ reaction is satisfactorily reproduced in absolute value.

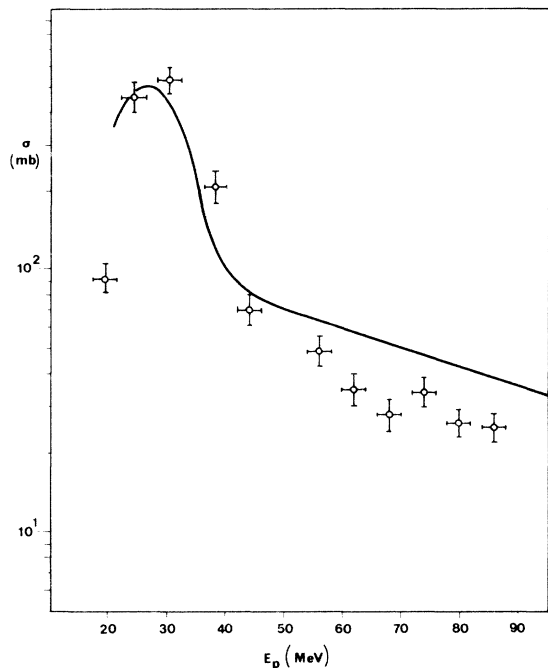
All the calculations of the reactions induced on ^{88}Sr have been done by assuming $\phi = 0.1$. However, the absolute value of the cross sections of those processes to which α particle emission does not contribute is only slightly affected by the value assumed for ϕ .

B. Analysis of ^{89}Y excitation functions and of the spectra of protons and α particles measured at incident proton energy of 61.5 MeV

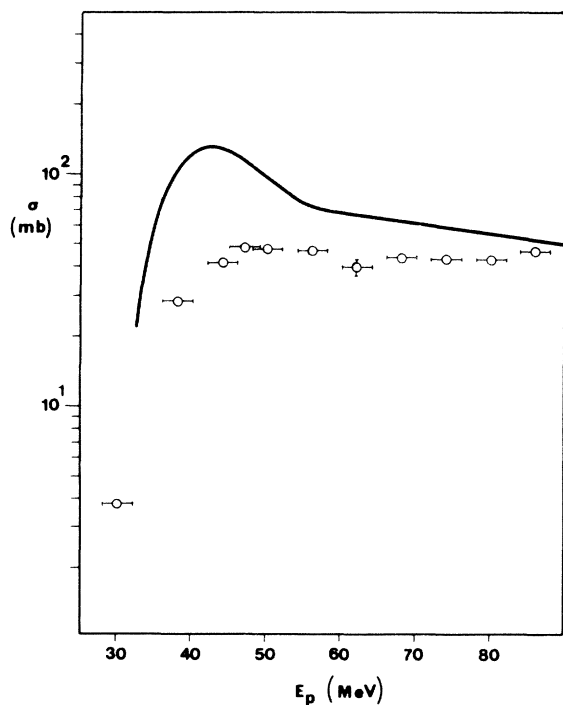
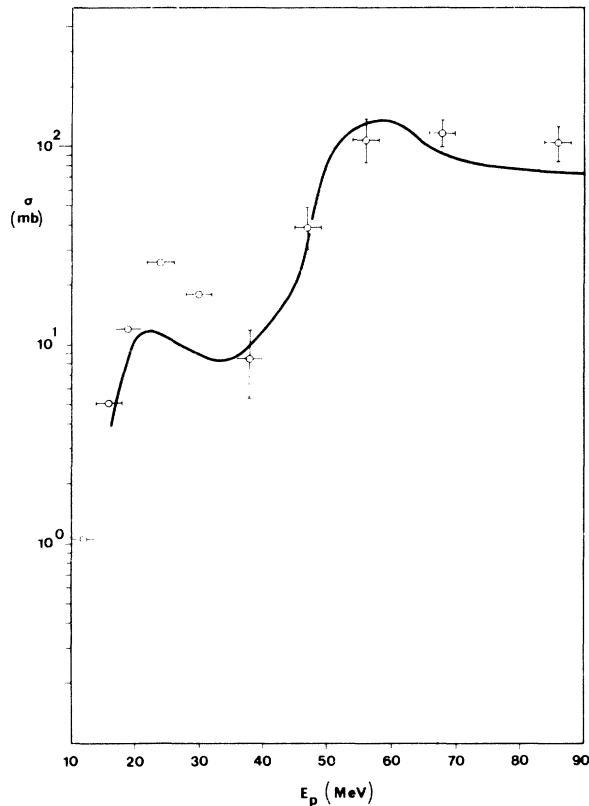
The absolute yield and the shape of the calculated energy distribution of the α particles which were measured by Bertrand and Peelle at 61.5 MeV in-

cident proton energy depend sensitively on the choice of the coefficient ϕ . Analysis of these data (see Fig. 19) seems to indicate for ϕ the value 0.05. All the calculations discussed in this subsection have been performed by assuming for ϕ this value though this determination for ϕ is somewhat less reliable than the one obtained for instance in the case of ^{90}Zr excitation functions being based on a single measurement at a fixed energy.

The agreement between theoretical calculations and experimental excitation functions of (p, xn) reactions ($x = 1, 3, 4$) is rather good up to the maximum energy considered. In the case of the (p, n) reaction, better agreement between the theory and experimental data was reported in previous papers^{5,14} by using a best fit procedure. The present calculation slightly overestimates the experimental cross section in the tail region due to the assumption, in this paper, of equidistant single nucleon states at energies exceeding the Fermi energy. The composite nucleus state densities are reduced

FIG. 21. As Fig. 4, for the $^{90}\text{Zr}(p, 2n)$ reaction.

in comparison with the ones calculated in the previous papers (their reduction is greater than the one of the residual nucleus state densities) thus increasing the calculated cross sections. The analysis of the accompanying excitation functions,

FIG. 22. As Fig. 4, for the $^{90}\text{Zr}(p, 2pn)$ reaction.FIG. 23. As Fig. 4, for the $^{90}\text{Zr}(p, 2p2n)$ reaction.

however, seems to indicate that the new assumption does not introduce a systematic deviation between experiment and theory.

The agreement of the (p, p_xn) measured and calculated excitation functions ($x=2, 3, 4, 5$) is satisfactory in all cases, even at the highest energies. Also the spectral distribution of protons and α particles emitted in proton bombardment of Y at 61.5 MeV is very satisfactorily reproduced both in shape and intensity.

C. Analysis of ^{90}Zr excitation functions

These data are particularly suited to a study of the decay through α channels of the excited composite nucleus. In the case of the excitation functions of the reactions $(p, xpyn)$, $x=2, 3$, the contribution of the $[p, \alpha(x-2)p(y-2n)]$ is the only one energetically allowed at the lowest energies giving rise to a first maximum followed by a valley and a second rise when the emission of individual nucleons becomes energetically possible.

The $(p, xpyn)$ excitation functions for $x=4$ and $y \geq 4$ show a first maximum attributable to the reaction $[p, 2\alpha(y-4n)]$. Beyond this maximum a

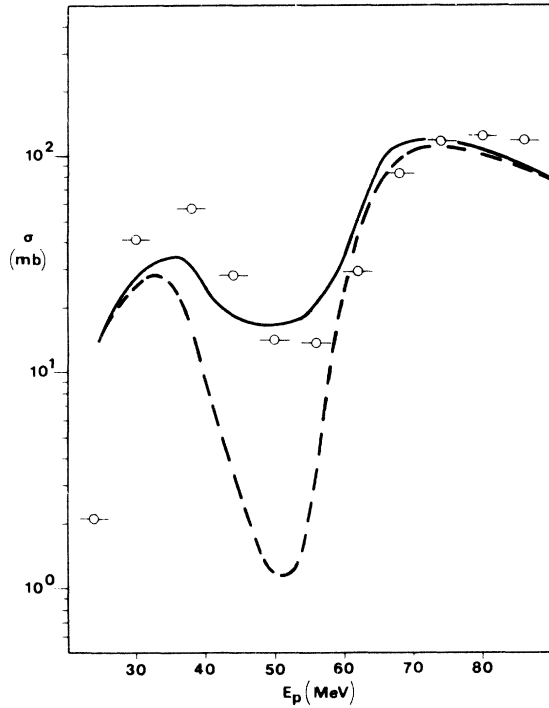


FIG. 24. As Fig. 4, for the $^{90}\text{Zr}(p, 2p3n)$ reaction. The dashed line has been calculated with $\phi = 0$ implying no preequilibrium emission of α particles. See discussion in text.

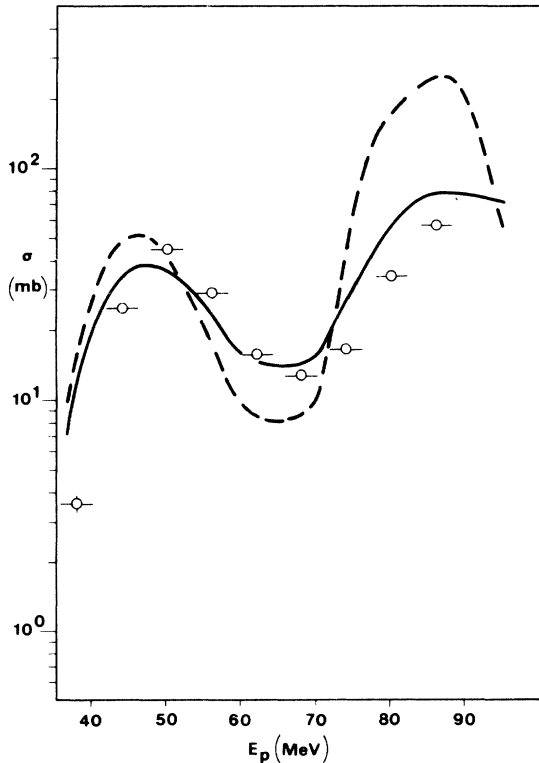


FIG. 25. As Fig. 5, for the $^{90}\text{Zr}(p, 2p4n)$ reaction.

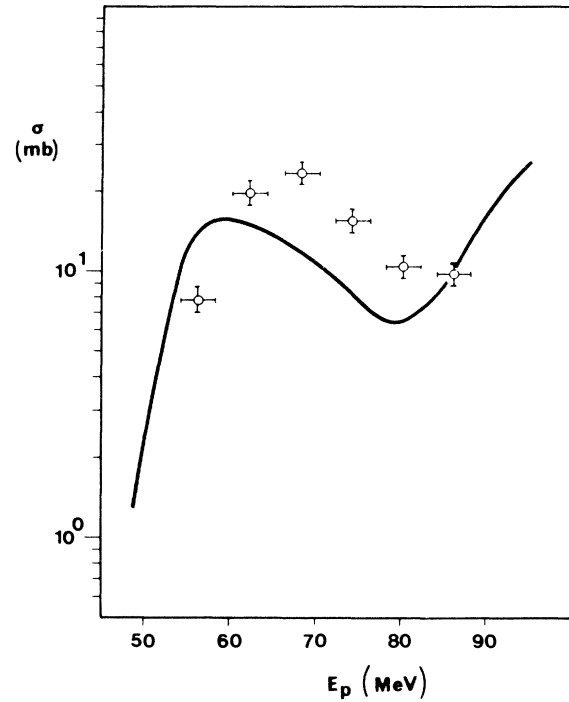


FIG. 26. As Fig. 4, for the $^{90}\text{Zr}(p, 2p5n)$ reaction.

valley follows and a second rise due to the reaction $[p, \alpha 2p(y-2n)]$. In the energy range considered the contribution of reactions to which only individual nucleon emissions contribute is not energetically possible.¹³

The analysis of these data suggested the value

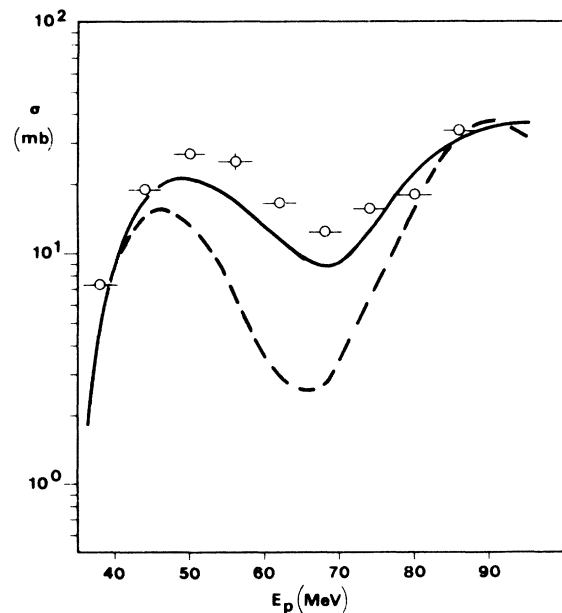


FIG. 27. As Fig. 24, for the $^{90}\text{Zr}(p, 3p3n)$ reaction.

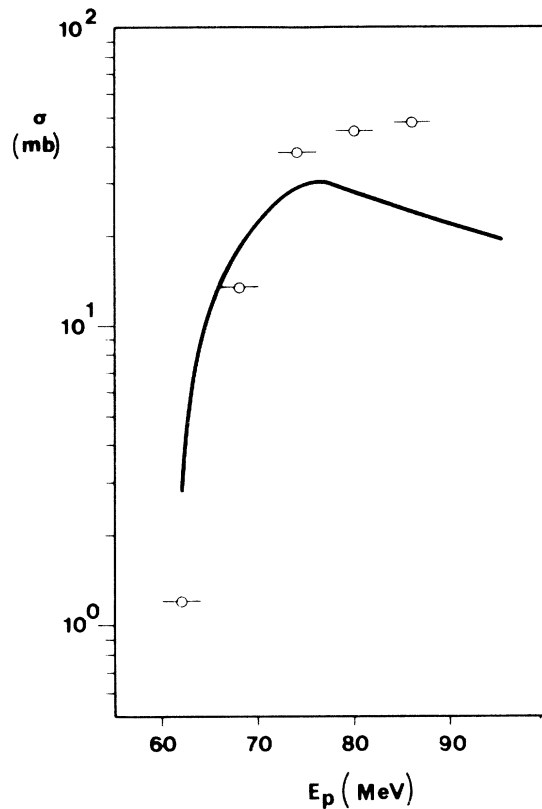


FIG. 28. As Fig. 4, for the $^{90}\text{Zr}(p, 3p5n)$ reaction.

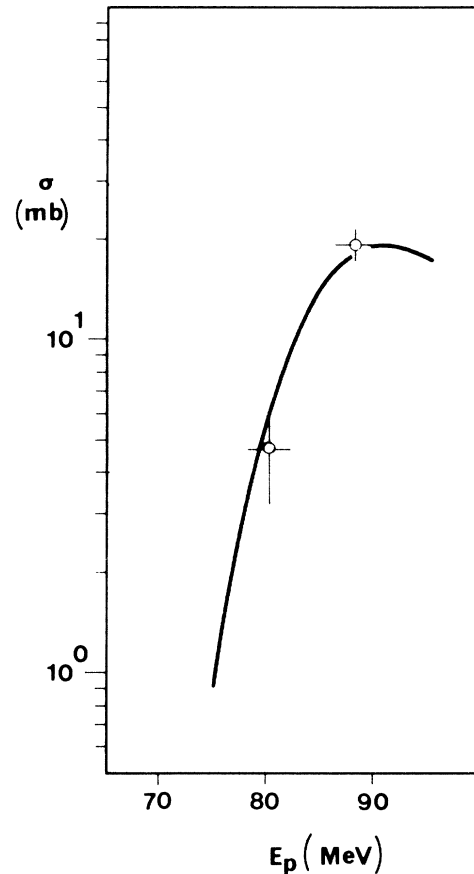


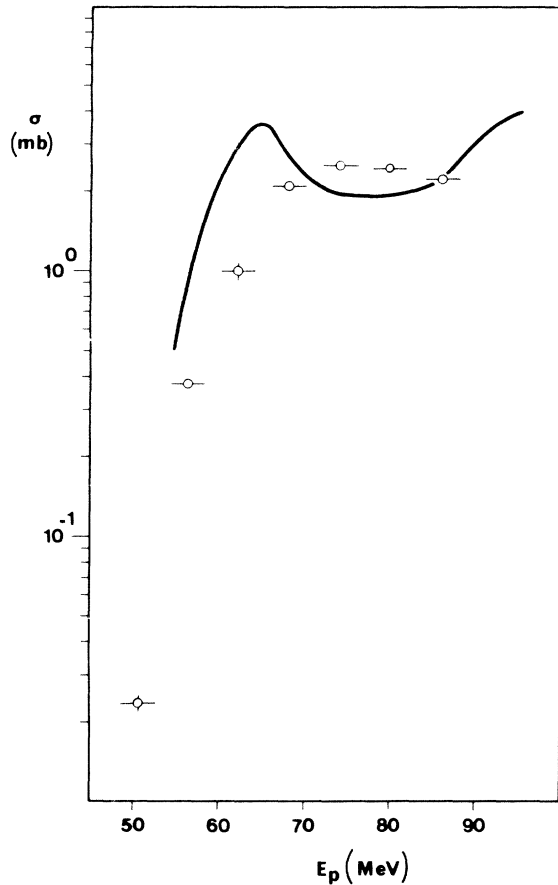
FIG. 29. As Fig. 4, for the $^{90}\text{Zr}(p, 3p6n)$ reaction.

0.15 for ϕ . Calculations have also been performed by assuming $\phi = 0$. Some typical results are compared with the experimental data in Figs. 24, 27, and 31. If $\phi = 0$ there is no possibility of preequilibrium emission of α particles; only evaporated α particles contribute to the reactions. The comparison with the experimental data of these last calculations shows that the contribution of preequilibrium emitted α particles is predominant in the valley which follows the first maximum.

At the first maximum the contribution of evaporated α particles is not negligible although the theoretical calculation of the $(p, 2\alpha)$ reaction shows an almost vanishing probability for both α particles to be evaporated. The (p, n) and $(p, 2n)$ excitation functions are satisfactorily reproduced both in shape and absolute value though in the tail region the calculated $(p, 2n)$ cross sections overestimate the experimental ones by about 30%. Among all the considered reactions the calculated $(p, 2pn)$ excitation function is the one which most conspicuously deviates from the experimental results. To interpret this result it is necessary to recall that in the 30–50 MeV incident proton energy range the main contribution to the $(p, 2pn)$ reaction is evaporation from the compound nucleus.

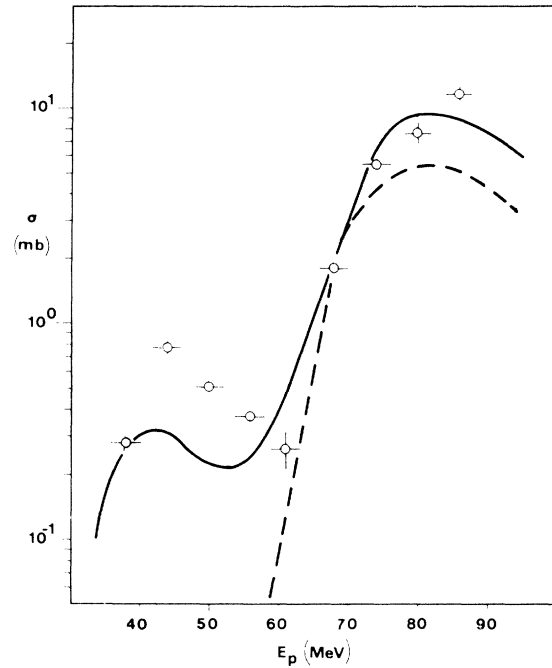
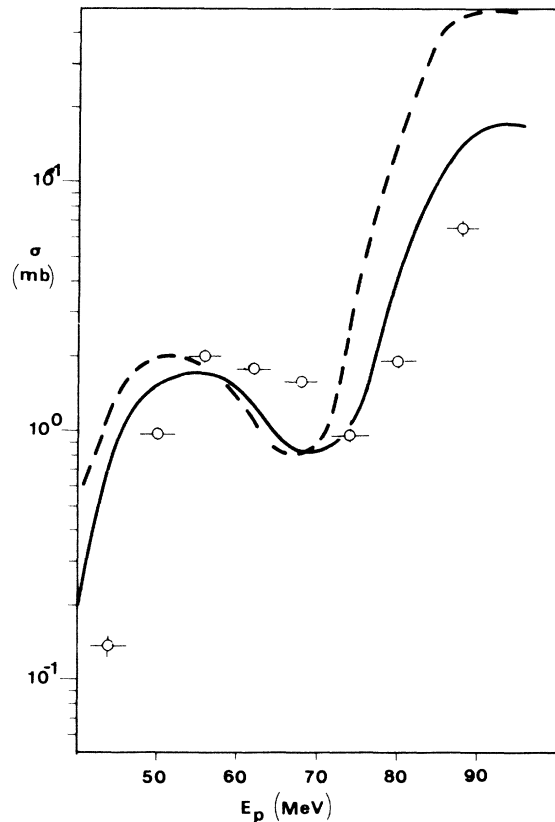
It might also be noted that the peak in the calculated excitation function (Fig. 22) is absent in the ^{88}Sr case (Fig. 8). There, the proton binding energy makes the evaporation of two protons and a neutron from the compound nucleus very unlikely. Here, we attribute the disagreement to the use of the level density parameter, $a = (A/8) \text{ MeV}^{-1}$, which leads to an overestimation, especially at rather low excitation energies, of the level density of the ^{90}Zr nucleus which has a closed shell of 50 neutrons and a closed subshell of 40 protons. The yield of the first evaporated protons is thus overestimated leading to a cross section for the $(p, 2pn)$ reaction greater than the measured one at energies lower than about 50 MeV. This is essentially the same reason for the disagreement between the calculated $(p, 2p2n)$ cross section and the experimental one in the region of the first maximum.

In fact, by using average a values, as we do, we expect to underestimate the ratio between the level density of ^{87}Y and ^{90}Nb , if shell effects are present, thus underestimating the (p, α) reaction cross section. The influence of shell effects gradually disappears with increasing excitation energy of

FIG. 30. As Fig. 4, for the $^{90}\text{Zr}(p, 4p3n)$ reaction.

the residual nucleus after the first α or proton evaporation or when preequilibrium decays become important. We thus obtain a satisfactory agreement between experimental data and calculations in the case of $(p, 2p3n)$, $(p, 2p4n)$, and $(p, 2p5n)$ reactions and, at incident proton energies greater than ≈ 50 MeV, as well as for $(p, 2pn)$ and $(p, 2p2n)$ reactions. The agreement of calculated and experimental excitation functions is satisfactory in the case of $(p, 3p3n)$, $(p, 3p5n)$ and $(p, 3p6n)$ reactions. Of particular note are the results that have been obtained in the case of $(p, 4pxn)$ reactions ($x=3, 4, 5, 6$). The measured cross sections range in value from about 0.1 to about 10 mb.

The effect to be reproduced by the statistical calculations we report is of the order of one event per thousand cascades, a very small effect indeed. The quality of the fit is about the same as in previous calculations, thus indicating that the model and the parameters utilized allow a very detailed and precise analysis of the deexcitation of the composite nucleus. This is indeed the main conclusion we draw from all the previously shown comparisons of experimental data and theoretical

FIG. 31. As Fig. 24, for the $^{90}\text{Zr}(p, 4p4n)$ reaction.FIG. 32. As Fig. 5, for the $^{90}\text{Zr}(p, 4p5n)$ reaction.

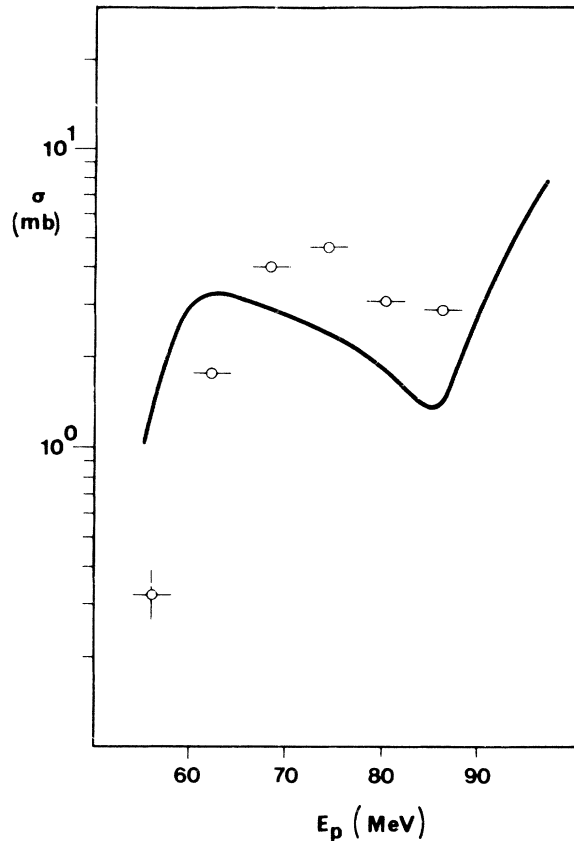


FIG. 33. As Fig. 4, for the $^{90}\text{Zr}(p, 4p6n)$ reaction.

calculations, a conclusion which is not altered by the occasional small discrepancies we have discussed. The values we found for ϕ are consistent with the assumptions we introduced and discussed at length above.

Finally, Kantelo and Hogan¹³ reported the fractional probability of emission of various combinations of charged particles; these are compared with the results of the present calculation in Fig. 34. Most of the curves are in excellent agreement with the experimental data. Small differences probably arise from a shift in the experimental curves by 1–2 MeV in either direction because of an inability to estimate the position of the missing experimental excitation functions. For this reason, we feel the deviations of the calculation from experiment in Fig. 34 do not represent errors in the calculated fractional probability of emission of the combinations of charged particles.

Only the probability of two proton emission seriously differs from the experimental data at proton energies from 30 to 50 MeV. This arises entirely from an overestimate of the $(p, 2pn)$ excitation function, discussed above, and is attributed to the use of average level densities in the magic ^{90}Zr nu-

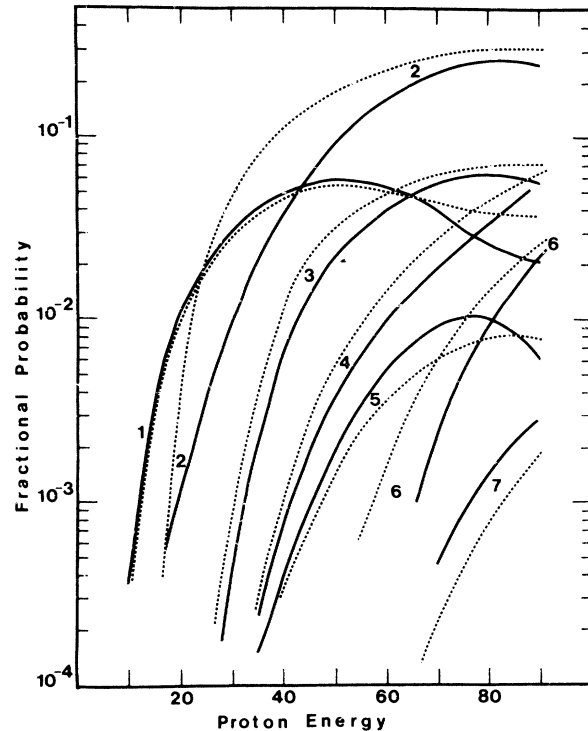


FIG. 34. A comparison of the calculated (dashed line) and experimental (full line) fractional probabilities of emission of various combinations of charged particles. Line 1, $(p, \alpha xn)$; line 2, $(p, 2pxn)$; line 3, $(p, p\alpha xn)$; line 4, $(p, 3pxn)$; line 5, $(p, 2\alpha xn)$; line 6, $(p, \alpha 2pxn)$; line 7, $(p, 4pxn)$.

cleus.

We do not attribute great importance to the differences we found in the values of ϕ in the three reactions considered. The ^{88}Sr and ^{90}Zr data are both consistent with $\phi = 0.15$. In the case of ^{89}Y the $\phi = 0.05$ value was obtained by analyzing only one spectral distribution at a given energy.

No theories exist at present which could predict reasonable values for ϕ . It should be also mentioned that the values we quote for ϕ depend on the naive assumption that the α particle single state density inside the nucleus equals one quarter of the single nucleon state density.^{1,24,26}

In our opinion the most important result concerning α particle emission is that the analysis of the data seems to confirm that the α particles emitted in preequilibrium reactions are preformed inside the nucleus. The previous evidence for such a reaction mechanism was restricted to rather low excitation energies. Our analysis seems to indicate that, in the case of $A \approx 90$ nuclei this reaction mechanism is responsible for emission up to excitation energies of about 100 MeV.

The decays in neutron and proton channels are

almost unaffected by the values assumed for ϕ . In the calculations we reported in these cases, essentially no free parameters are present. The excellent agreement we found up to excitation energies of about 100 MeV confirms and extends the validity of the model and the parameters we suggested.^{1,14-16,28}

V. DISCUSSION OF NUCLEON MEAN FREE PATHS

It was soon apparent, from attempts to deduce the decay rates for exciton-exciton interactions from the analysis of data [e.g., excitation functions of (p, n) reactions,^{5,14} absolute cross sections of (n, p) reactions at $E_n \approx 14$ MeV (Ref. 33) and spectral distributions of neutrons and protons in (n, n') and (p, n) and (p, p') reactions^{34,35}], that the estimated mean free path of a nucleon having energy greater than 30 MeV inside the nucleus, a quantity with a weak energy dependence up to energies of the order of 100 MeV, is greater than the value expected on the basis of calculations based on the Fermi gas model and the use of free nucleon-nucleon cross sections.³⁶ To give a numerical estimate, the value is about 16.7 fm, i.e., greater than the rms diameter of a heavy nucleus. This finding suggested nuclei might be nearly transparent to incident projectiles. To investigate this point a formula was derived, in the framework of the exciton model, for the absorption cross section and it was shown that correct values for this quantity could be obtained if, in a sharp surface approximation, the low density regions of the nucleus were included in the absorbing nuclear volume.¹⁵ It is obvious that the increase of the nuclear radius can counteract, in calculations like the ones we refer to, an abnormally large nucleon mean free path. The physical justification for the above quoted result rested on the consideration that detailed calculations did not show any appreciable increase of the nucleon mean free path in the low density nuclear regions since the reduced nuclear density is largely counteracted by the increased average nucleon-nucleon cross section.^{14,15}

In addition to these considerations, the present calculations confirm the large value previously found for the nucleon mean free path, by indicating that this large mean free path allows one to repro-

duce correctly, at each considered energy, both the yield of particles emitted in the preequilibrium stage and the yield of evaporated particles.³⁷ In fact, it is an obvious consideration that an overestimation of the nucleon mean free path should enhance the fraction of preequilibrium emissions and reduce the fraction of evaporations contributing to a given process. The reverse occurs if the nucleon mean free path is underestimated. To provide a more convincing proof of these statements all the calculations previously discussed in Sec. IV have also been done by reducing by a factor 4 the nucleon mean free path, i.e., using the value for this quantity one deduces by means of calculations based on the Fermi gas model and free nucleon-nucleon cross sections. Some of the results we obtained are shown in Figs. 5, 9, 13, 14, 18, 25, and 32. In all the cases, when this short value for the mean free path was used, the fraction of events leading to the compound nucleus was overestimated and the yield of preequilibrium emissions underestimated. As a consequence: (a) in the case of the excitation functions of complex reactions the maximum was in all cases greatly overestimated while in the tail regions the calculated cross sections were much smaller than the measured ones; (b) in the calculation of the spectra of the protons emitted in the $^{89}\text{Y}(p, xp)$ reaction the low energy evaporative peak was overestimated while the hardest part of the spectrum was underestimated. This result is the same that is found by analyzing the same data we have considered in the present paper by means of the Monte Carlo intranuclear cascade code VEGAS^{8, 9, 13} which utilizes mean free paths of the order of the ones we used in this second series of calculations.

VI ACKNOWLEDGMENTS

Thanks are due Dr. P. Oblozinsky and Dr. E. Betak for enlightening discussions and to Professor G. Tagliaferri for a careful and critical reading of the manuscript. Two of us (E.G. and J.J.H.) wish to thank the North Atlantic Treaty Organization for a travel grant. The experimental work was made possible by a grant from the National Research Council of Canada.

¹E. Gadioli and L. Milazzo Colli, *Lecture Notes in Physics* (Springer, Berlin, 1973), Vol. 22, pp. 84. E. Gadioli, E. Gadioli Erba, L. Sajo Bohus, and G. Tagliaferri, *Nuovo Cimento Riv.* 6, 1 (1976); E. Gadioli, *Nukleonika*, 21, 385 (1976).

²M. Blann, *Annu. Rev. Nucl. Sci.* 25, 123 (1975).

³D. Agassi and H. A. Weidenmuller, *Phys. Lett.* 56B,

305 (1975); D. Agassi, H. A. Weidenmuller, and G. Mantzouranis, *Phys. Rep.* 22C, 147 (1975); G. Mantzouranis, H. A. Weidenmuller, and D. Agassi, *Z. Phys.* A276, 145 (1976).

⁴W. W. Bowman and M. Blann, *Nucl. Phys.* A131, 513 (1969); M. Blann and F. M. Lanzafame, *ibid.* A142, 559 (1970).

- ⁵C. Birattari, E. Gadioli, E. Gadioli Erba, A. M. Grassi Strini, G. Strini, and G. Tagliaferri, Nucl. Phys. A201, 579 (1973).
- ⁶E. Gadioli and E. Gadioli Erba, Nucl. Phys. A256, 414 (1976).
- ⁷J. C. Brodovitch, J. J. Hogan, and K. I. Burns, J. Inorg. Nucl. Chem., to be published.
- ⁸G. B. Saha, N. T. Porile, and L. Yaffe, Phys. Rev. 144, 962 (1966).
- ⁹D. R. Sachdev, N. T. Porile, and L. Yaffe, Can. J. Chem. 45, 1149 (1967).
- ¹⁰J. J. Hogan, Phys. Rev. C 6, 810 (1972).
- ¹¹P. Jahn, H. J. Probst, A. Djaloeis, W. F. Davidson, and C. Mayer B6ricke, Nucl. Phys. A209, 333 (1973).
- ¹²J. Bisplinghoff, J. Ernst, H. Machner, T. Mayer Kuchuck, and R. Schanz, Nucl. Phys. (to be published).
- ¹³M. V. Kantelo and J. J. Hogan, Phys. Rev. C 14, 64 (1976); M. V. Kantelo, Ph.D. thesis, McGill University, Montreal, Quebec, Canada, 1975 (unpublished).
- ¹⁴E. Gadioli, E. Gadioli Erba, and P. G. Sona, Nucl. Phys. A217, 589 (1973).
- ¹⁵E. Gadioli, E. Gadioli Erba, and P. G. Sona, Nuovo Cimento Lett. 10, 373 (1974).
- ¹⁶E. Gadioli and E. Gadioli Erba, Acta Phys. Slov. 25, 126 (1975).
- ¹⁷F. E. Bertrand and R. W. Peelle, Oak Ridge National Laboratory Report No. ORNL 4450, 1969 (unpublished).
- ¹⁸F. K. McGowan, W. T. Milner, H. J. Kim, and W. Hyatt, Nucl. Data A7, No. 1 (1969).
- ¹⁹J. J. Menet, E. E. Gross, J. J. Malanify, and A. Zucker, Phys. Rev. C 4, 1114 (1971).
- ²⁰D. A. Newton, S. Sarkar, L. Yaffe, and R. B. Moore, J. Inorg. Nucl. Chem. 35, 361 (1973).
- ²¹K. Chen, Z. Fraenkel, G. Friedlander, J. R. Grover, J. M. Miller, and Y. Shimamoto, Phys. Rev. 166, 949 (1968).
- ²²K. Chen, G. Friedlander, and J. M. Miller, Phys. Rev. 176, 1208 (1968).
- ²³K. Chen, G. Friedlander, G. D. Harp, and J. M. Miller, Phys. Rev. C 4, 2234 (1971).
- ²⁴L. Milazzo Colli and M. G. Braga Marcazzan, Nuovo Cimento Riv. 3, 535 (1973).
- ²⁵I. Dostrovsky, Z. Fraenkel, and G. Friedlander, Phys. Rev. 116, 683 (1959).
- ²⁶L. Milazzo Colli and M. G. Braga Marcazzan, Phys. Lett. 38B, 155 (1972); Nucl. Phys. A210, 297 (1973); L. Milazzo Colli, M. G. Braga Marcazzan, M. Milazzo, and C. Signorini, Nucl. Phys. A218, 274 (1974); A. Chevarier, N. Chevarier, A. Demeyer, G. Hollinger, P. Pertos, and Tran Minh Duc, Phys. Rev. C 11, 886 (1975).
- ²⁷E. Betak and J. Dobeš, Report of the Institute of Nuclear Physics, Czechoslovak Academy of Sciences, 1976 (unpublished).
- ²⁸E. Gadioli, E. Gadioli Erba, and G. Tagliaferri, Phys. Rev. C 14, 573 (1976).
- ²⁹T. Ericson, Adv. Phys. 9, 423 (1960).
- ³⁰A. H. Wapstra and N. B. Gove, Nucl. Data A9 (Nos. 4 and 5), 268 (1971).
- ³¹W. D. Myers and W. J. Swiatecki, Ark. Fys. 36, 343 (1967).
- ³²P. E. Nemirovski and Yu. V. Adamchuck, Nucl. Phys. 39, 551 (1962).
- ³³M. G. Braga Marcazzan, E. Gadioli Erba, L. Milazzo Colli and P. G. Sona, Phys. Rev. C 6, 1398 (1972).
- ³⁴D. Hermsdorf, S. Sassonov, D. Seeliger, and K. Seidel, in *Proceedings of the International Conference on Nuclear Physics, Munich, 1973*, edited by J. de Boer and H. J. Mang (North-Holland, Amsterdam/American Elsevier, New York), Vol. I, pp. 514, 518.
- ³⁵C. Kalbach Cline, Nucl. Phys. A210, 590 (1973).
- ³⁶The discussion reported in this section is restricted to the results one obtains by analyzing the experimental data by means of the exciton model. Attention will be paid to the results obtained by means of other theoretical models only when they refer to the same data we have considered in this paper. For the sake of objectivity one must be reminded that according to M. Blann [Nukleonika 21, 335 (1976)] by utilizing the Hybrid and Geometry Dependent Hybrid Models one reaches conclusions at variance with the ones arrived at in this section. It is our opinion that a detailed comparison and discussion of the different models utilized to describe the preequilibrium decay of an excited nucleus is demanded; we think however that this discussion has to be deferred to another place since this work was not intended to obtain a better theoretical understanding of the foundations of preequilibrium models but just to explore the capability of one of these, the exciton model, in reproducing at the same time the cross sections of many competing reactions proceeding through composite nuclei excited up to ≈ 100 MeV. On the other hand, it is our opinion that material like the one collected in this paper will greatly help in clarifying the theoretical ideas in the field of nonequilibrium statistical processes.
- ³⁷E. Gadioli, E. Gadioli Erba, G. Tagliaferri, and J. J. Hogan, Phys. Lett. 65B, 311 (1976).